# Soil geochemistry characterization and climate vulnerability projections to bark beetle-pine dynamics at “Volcán Nevado de Colima”, Mexico.

## A high elevation forest study case


Utrecht University

Earth Science and Geoscience Faculty

Master Thesis research

Alonso Villalobos

Supervisor: Jack Middelburg

Student number: 6692672

a.villalobosechevarria@students.uu.nl

## Acknowledgments:

This work represents the culmination of more than one year of work for me. Being by myself abroad when the covid situation started felt hard, this research thesis gave me the enormous opportunity of creating scientific research in a place that I have nothing but love. Creating the project from scrap and according to the topics I saw in my masters was a great challenge, but the reward and the connections I have done made it all worth it.

To Pilar and Jaime, thank you for everything you have done for me, your constant support has given me the means of constructing myself as a better and more prepared person and has given me the responsibility to make my environment a better place

To my parents, your constant support meant and means everything for me, during the hard days you were my main pillar and you always kept me pushing forward towards the realization of this and all of my projects. Also, enormous thanks to my older brothers, who maybe didn't help much in the project but made my days better for sure. This includes my big brother's extension, aka my nephew.

To Jack, thank you for supporting the creation of this research without any hesitation since day one, and for being my supervisor for this thesis project abroad. Dankuwel

To Sonia Navarro, Pepe Villa and the mountain management thank you for offering me all your support and the means to work my soil samples in Universidad de Guadalajara laboratories as well as for inviting me to be part of the research group of the National Park.

To Caro, thank you for all your support and for letting me store all of my mountain gear and soil samples in your house. You made my time staying in Guadalajara for my fieldwork and lab work one of the best times I've had.

To Sergio, gracias Concilieri, you have been a true guide in this project and in all of my European time.

# Contents

## Summary:

Characterization of soil components and a weather and climate vulnerability analysis at the Volcanic Complex of Colima, Mexico was conducted. The study was performed through varying forest structures and altitudes for the *Dendroctonus Adjuntus-Pinus Hartwegii* natural dynamic. Three main forest structures were defined according to the outbreak and post-migration times. (green: no beetle outbreak at the site; yellow and red: not long ago beetle outbreak resulting in yellow and red needles in pines; and grey: long ago post-outbreak, deriving in pines with no more needles and fallen branches). Geochemical components varied across these structures and altitudes in different ways. Main results tell that organic matter, potassium ion, sodium ion, and humidity content had greater concentrations across the yellow and red forest structures, while nitrogen, phosphorus, calcium ion, and magnesium ion had the greatest concentrations across grey structures.

The study exhibited that weather parameters appear to be drivers for this natural dynamic at the VCC, where a decrease in precipitation and relative humidity, along with increases in air temperature and radiation correlated to the late outbreaks and high forest vegetation transitions. The cumulative generated data indicates that the dynamic occurs mostly in the altitudinal range comprehended between 3400 and 3800 masl.

## Glossary:

masl: Meters above sea level

VCC: Volcanic Complex of Colima

DEM: Digital Elevation Model

PCC: Pearson Correlation Coefficient

PCA: Principal Component Analysis

ppm: parts per million

GCV: Gross change of vegetation

G1: altitudinal zone 1

G2: altitudinal zone 2

G3: altitudinal zone 3

G4: altitudinal zone 4

CEC: Cation exchange capacity

AARH: Annual average relative humidity

AAAT: Annual average air temperature

AARad: Annual average radiation

OM: Organic matter

EC: electrical conductivity

## Introduction:

Parque Nacional Volcán Nevado de Colima or Volcanic Complex of Colima (VCC) is a National Park situated between the states of Jalisco and Colima, Mexico, in an area known as the neovolcanic belt. The park hosts “Volcan de Colima” an active volcano with an altitude of 3960 masl, and “Nevado de Colima” an ancient volcano massif with an altitude of 4270 masl (Lugo-Hubp et al. 1992). Above 3000 masl the primary and dominant vegetation is composed mainly of the pine species *Pinus Hartwegii* (Lauer, 1973; Lauer and Klaus, 1975), this pine species has a natural dynamic in the mountain with the bark eating beetle *Dendroctonus adjuntus*, this natural dynamic between conifers and beetles is of great importance to the forests and mountains (Jonášová et al. 2004; Jonášová et al. 2007).

Pinus Hartwegii is found distributed across the neo volcanic belt in the Mexican high mountains, this pine species represents the altitudinal limit of tree vegetation known as timber line for these high mountains and volcanoes such as it happens in the VCC (Lauer, 1973; Lauer and Klaus, 1975). Because the pine is isolated in the high mountains and because of its tolerance to cold environments the species is of great importance and highly vulnerable to changing conditions such as climate change (Viveros et al. 2007).

Bark-eating beetles infestations in pine trees have considerably increased over the last decades, these infestations have induced high tree mortality among the pine forests (Mikkelson et al. 2013). Several authors (Mikkelson et al. 2013; Franceschi et al. 2005; Vite, 1961; Solheim, 1988) have studied relationships between bark beetles and conifers and their dynamics and relationships, however, no evidence has been analyzed for the VCC natural dynamic between Pinus Hartwegii and Dendroctonus Adjuntus. Therefore the importance of documenting evidence of this natural dynamic in the National Park.

In areas where pine density is higher (between 3300 and 3900 masl), the dynamic between bark beetle and their host has been much more noticeable, big patches of pines sectors with yellow and red needles and grey sectors of death pines that lost all needles and branches can be seen across all of the high elevations of the mountain (figure 1). As a result of this interaction, much of the soil coverage in the high altitudinal zones are under different processes that leave the soil more prone to changes in its composition. VCC and their *Dendroctonus Adjuntus* migrations and dynamic with Pinus Hartwegii appear to be increasing since the last half-decade (figure 1), Creeden et al. 2013 stated that climate and weather can act as a driver of this interaction. Thus, this whole dynamic along with the soil and its components appears to show vulnerability towards climate change.

### Pine-beetle dynamics

Bark beetles enter the pines through the bark. After the beetles enter through the bark, they create tunnels called galleries seeking the tree’s phloem (figure 2). This leads them to the secondary phloem or cambial zone (Franceschi et al. 2005), where

resin reserves are depleted and the phloem and cambium translocation are destroyed (Vite, 1961; Solheim, 1988). This process leads to pine mortality (figures 1 & 2), consequently end up releasing material (branches and needles) into the soil. As tree material starts to fall and furtherly decompose, it is expected to increase concentrations in carbon, phosphorus, and certain cations. (Yavitt and Fahey 1986). For the organic matter in the soil, the increase in dissolved organic carbon might change at different rates since rhizodeposition and mycorrhizal interactions with dead trees decrease overall (Mikkelson et al. 2013). In sites where bark beetle migrated the tree canopy decreases, allowing moisture to change at different rates at different altitudes (Mikkelson et al. 2013). Hence, soil biogeochemical cycles and components should change after *Dendroctonus adjuntus* migrations at VCC.

Bark beetle outbreaks in VCC appear to be related to climate change, the climate and weather factors exert an influence throughout three main factors which are considered to be drivers for bark beetle outbreaks, 1) adaptive season of the bark beetle to warmer periods increases. 2) There is a decrease in the cold-induced mortality, and 3) drought might create stress on host tree species (Creeden et al. 2013).

Changes in air temperature, relative humidity, precipitation, and radiation can derive in a greater capacity of the bark beetle *Dendroctonus adjuntus* to adapt to the mountain seasons, cold-induced mortality can decrease at warmer periods for the bark beetle, and local pine species *Pinus Hartwegii* can be under stress due to drought conditions (Bentz et al. 1991; Logan and Bentz, 1999; Logan and Powell, 2001)

*Figure 1. Forest structures: trees with yellow and red needles (left) and Grey structure site (right)*

*Figure 2. At left Dendroctonus Adjuntus larvae. At middle: Tunnel galleries created by beetles. At right: Sapwood occlusions from a dead pine*

## Region of study:

The National Park is the region of the VCC above 2500 masl (Park decreet, 1926). The northern part of the complex holds “Nevado de Colima” with a height of 4270 masl and 2700 meters of prominence, formed during the Late Pleistocene (Lugo-Hubp et al. 1992). The southern part of the volcanic complex is occupied by “Volcan de Colima” (Figure 3), with an altitude of 3960, originated in the Holocene from a wide-open caldera. It is one of the Mexican highly active volcanoes (Lugo-Hubp et al. 1992). Within the volcanic complex 10 species of woody vegetation are found, the upper zones of the mountain are mostly occupied by species of the Pinaceae family (*Pinus Hartwegii, Pinus pseudostrobus, Abies religiosa*), Fagaceae family (*Quercus Laurina*), and Cupressaceae family (*Cupressus Lindley*) (Miranda et al. 2009).

There are five meteorological stations within the volcanic complex, four of them are found in lower sites distributed along with the complex while the fifth one is found in the upper zone of “Nevado de Colima” at 3430 masl

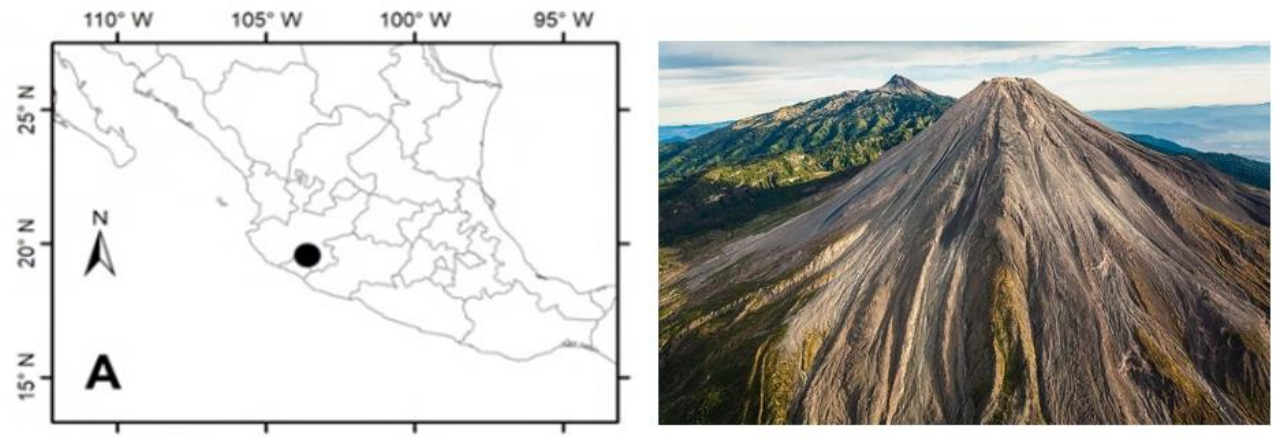


*Figure 3. Geographical localization of VCC at left. Right picture, Sergio Tapiro's photo of the VCC from south to north. Volcan de Colima at south, and Nevado de Colima at north*

## Aim of the study:

The research aims to understand the natural dynamic of the pine-beetle in the high spectrum of the mountain by two main goals; 1) understand how soil components change throughout this interaction at different altitudes and 2) determine if the pine-beetle interaction is driven by climate and weather changes, therefore, the research is composed by two main chapters:

Chapter 1 has the objective of quantifying changes in the geochemical components of the alpine soil at different altitudes and within different forest structures. Three overall structures are considered, the first one corresponds to sites where there has not been the presence of the bark beetle, the second structure belongs to sites in which pines needles are yellow and red, and lastly the third structure has the pines completely grey without needles and much of the secondary branches. The structures are described by Mikkelson et al, 2013 as stages or transition phases after the beetle migrated to locations, associating times of approximately 0 to 4 years of post-outbreak for the second structure, and more than 4 years post-outbreak for the third structure for the grey sites approximately. The study will incorporate the measurements in the first soil horizon for 39 composed samples of organic matter content, total nitrogen, total phosphorous, soil cation capacity exchange, humidity content, soi temperature (in site), pH, and electrical conductivity.

Chapter 2 has the objective of determining the vulnerability of the pine-beetle dynamic towards climate change, by comparing transitions in forest structures to climate and weather data. The transition of vegetation interpretation will come from the processed imagery and interpretation of satellite images, while climate and weather data were provided from the upper station.

Both chapters should indicate how soil is related to this pine-beetle interaction, and how this interaction is vulnerable to climate and weather changes. The study should also give insight into how altitudinal conditions play an important role as well.

## Research questions:

How much and to which degree are soil components changing between forest structures and different altitudes as a result of the death of the pines?

How much of these dynamic late outbreaks in the VCC are driven by climate and weather change?

## My take-home message:

Before I started working on this thesis my knowledge about the bark beetle and its dynamic in the mountain was just what I had observed from my times in the mountain. The first time I visited the national park was in 2012, from there on, the migrations of the bark beetle have been very noticeable. Before I started working on the thesis I had the preconception that a forest must always be a green monoculture of pines. I saw this dynamic as a problem in which the beetle was a plague to the forest. Working on this thesis and getting to know people working in the mountain (mostly biologists) made me realize that it is a natural dynamic in which this particular beetle adapted to this particular pine species long ago and therefore plays an important role in the mountain.

Through literature research I found a considerable amount of research and work for this dynamic, there I saw how some authors even consider these dynamics a tool for forest restoration (Jonášová et al. 2007). About the same time, I started to get in contact with the park management authorities and with a local research group from Universidad de Guadalajara.

This research group along with park management has been in a legal struggle with some governmental agencies. These agencies use a traditional approach to the bark beetles outbreaks, which is to remove death biomass through sanitation practices. Currently, they are insisting with great perseverance to remove dead trees and biomass from locations that had bark beetle presence. On the other hand, the park management as well as the university research group have an approach to natural restoration and regeneration. The national park area has little anthropogenic perturbation as a result of its park status. This same status has permitted the park management to maintain dead pines from outbreak locations due that all *Pinus Hartwegii* population is above 3000 masl, all part of the National Park management.

This conflict sounded much in my head when I was reading a paper from (Jonášová et al. 2007), which mentions how this situation (referring to the different approaches) often leads to controversies about management policies against bark beetle in protected areas and national parks.

Without knowing it, my whole research could be useful for a natural restoration and regeneration approach, so my goal from the research mostly changed to the understanding of this dynamic through the soil components and finding and determining how changes in these components can be relevant for natural regeneration and part of a natural restoration process.

Lastly, the understanding of this dynamic in the mountain obeys a largely complex structure, with multiple parameters that affect the dynamic in various outcomes. By merging concepts and analysis I was interested in studying how the late outbreaks in the last decade can be influenced by climate and weather change in the mountain.

### Challenges:

Doing this research in the mid of the covid pandemic resulted in a whole challenge at the moment. I would have never expected to work on my project idea back to Mexico and continue being enrolled and working in the master's program. Besides the difficulty of the research, several challenges arose such as bureaucracy, looking for an external institution that supported the research, long waiting times for obtaining reactants (took me a long time to obtain some of them), and laboratory entrance permission for my soil analysis. At the same time, this challenge led me to join an amazing research work group, where I could learn and work within the mountain's management.

### Methodology limitations:

At the site, there is only one meteorological station in the high spectrum of the mountain. All region of the study was considered to have the same climate and weather conditions.

Satellite imagery is not complete, much of the year the whole mountain is covered in cloud cover and imagery cleanness. All the images were obtained between the months of December-February from the studied period (1989-2020).

Determination of organic matter was initially going to be determined by loss of ignition, but the laboratory that granted access to work soil samples did not have a muffle, so another analytical procedure was performed.

Kjeldahl technique for nitrogen calculates the total nitrogen, much of the literature explains how much of the increase of the nitrogen pool is in its inorganic form, with this technique there was no way to quantify the nitrogen pool in its components.

The same goes for the Bray P1 extract, which calculates the available phosphorus in the soil but does not determines its different forms.

Modeling future beetle migrations and forest transitions based on these migrations resulted in an extra challenge, as this is a complex dynamic and obeys a variety of parameters, such as micro climates in the mountain. Assuming the same climate conditions for all-mountain regions and create a model that predicts forest transitions based on this was too shallow and much more data and time are needed to assess a more complex and detailed model that predicts beetle outbreaks.

# Methods:

## Chapter 1. Geochemical components quantification of soil samples

The first step in the methodology was the determination of testing sites, location sites, and sampling had to be representative of a forest structure within a certain altitude (see table 1 and figure 5 below for sampling locations). In total, thirty-nine composed samples were retrieved from different sites between 3400 and 4000 masl. Each sample was made up of 7 extraction cores from different places within the site. Samples were stored in sealed plastic bags for further laboratory analysis. Samples were gathered using sampling soil protocols from Mason's (1992) methodology. Samples were collected between January and February.

*Figure 4. Soil core used in the field. At right: Core in soil and soil thermometer*

| Sample site | Coordinates (decimal) | | Stage (overall tree phase within site) Forest structure of the site | Altitude (masl) |
|---|---|---|---|---|
| | Latitude | Longitude | | |
| 1 | 19.589823 | -103.598619 | Yellow | 3423 |
| 2 | 19.588172 | -103.599830 | Green-yellow | 3441 |
| 3 | 19.581465 | -103.632732 | Red | 3522 |
| 4 | 19.580839 | -103.629961 | Grey | 3598 |
| 5 | 19.580264 | -103.630050 | Green sector with young regeneration | 3596 |
| 6 | 19.589248 | -103.593015 | Grey | 3359 |
| 7 | 19.588916 | -103.592010 | Yellow-red | 3334 |
| 8 | 19.568418 | -103.612824 | Yellow | 3807 |
| 9 | 19.569290 | -103.613375 | Yellow | 3766 |
| 10 | 19.568728 | -103.613852 | Green | 3779 |
| 11 | 19.570079 | -103.612845 | Grey | 3752 |
| 12 | 19.572491 | -103.611771 | Grey | 3695 |
| 13 | 19.575192 | -103.609623 | Green with some mistletoe | 3640 |
| 14 | 19.574816 | -103.608696 | Grey | 3628 |
| 15 | 19.571465 | -103.617767 | Green-yellow | 3900 |

| | | | | |
|---|---|---|---|---|
| 16 | 19.574179 | -103.620218 | Yellow-red | 3851 |
| 17 | 19.575968 | -103.619162 | Yellow | 3845 |
| 18 | 19.580185 | -103.616698 | Green | 3776 |
| 19 | 19.583120 | -103.614674 | Red-grey | 3763 |
| 20 | 19.580422 | -103.609244 | Yellow-red | 3722 |
| 21 | 19.585307 | -103.607493 | Green | 3625 |
| 22 | 19.583923 | -103.611114 | Yellow-red | 3765 |
| 23 | 19.584481 | -103.610944 | Green | 3760 |
| 24 | 19.585034 | -103.611372 | Yellow-red | 3847 |
| 25 | 19.585212 | -103.612217 | Grey | 3873 |
| 26 | 19.581426 | -103.602916 | Grey. Dead trees were withdrawn from site | 3464 |
| 27 | 19.581773 | -103.602345 | Grey with young reforestation at site | 3460 |
| 28 | 19.582203 | -103.603210 | Grey with young reforestation at site | 3470 |
| 29 | 19.569498 | -103.605438 | Green-yellow | 3888 |
| 30 | 19.570594 | -103.605580 | Green | 3831 |
| 31 | 19.571915 | -103.605088 | Yellow | 3775 |
| 32 | 19.572785 | -103.604790 | Green | 3739 |
| 33 | 19.574323 | -103.604062 | Grey | 3665 |
| 34 | 19.578736 | -103.601564 | Yellow-red | 3545 |
| 35 | 19.554395 | -103.614001 | Green-yellow | 3846 |
| 36 | 19.554625 | -103.611712 | Grey | 3862 |
| 37 | 19.59184 | -103.591556 | Grey | 3472 |
| 38 | 19.592044 | -103.590999 | Green | 3471 |
| 39 | 19.583458 | -103.600829 | Grey | 3441 |

*Table 1. Sampling sites locations*

Figure 5 shows sample sites locations within altitudinal lines every 100 meters and the forest structure of the sampling locations. Green forest structures are symbolized by triangles, yellow and red structures sites by circles, and grey structure sites by a diamond shape.

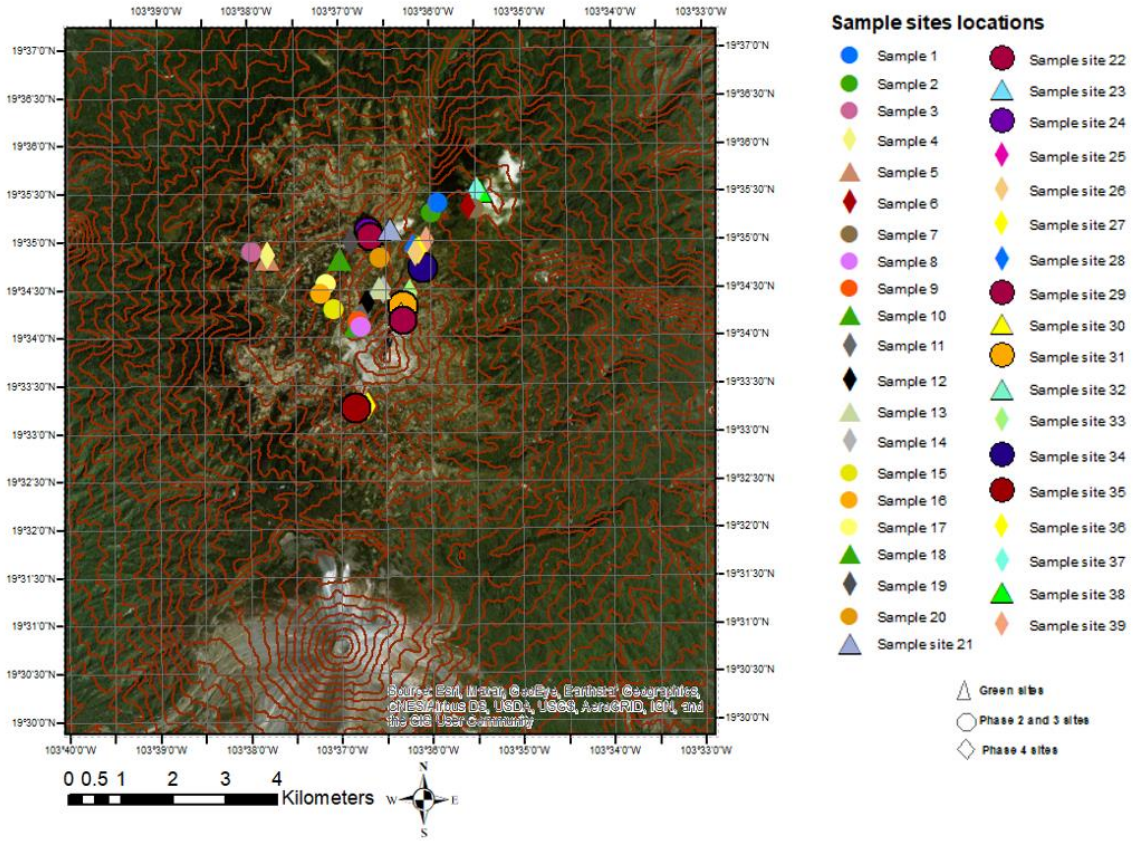


*Figure 5. Sampling locations at VCC*

## Components:

Components fluxes for the pine-beetle dynamic has been studied by several authors (Mikkelson et al. 2013; Prescott et al. 2000; Rosén et al. 1996; Griffin et al. 2011; Cullings et al. 2003; Huber et al. 2004), based on this, some trends of how the components can change in sites that had migration of the bark beetle can be expected, this changes of components between forest structures can vary in time and rate (Mikkelson et al. 2013) depending on site conditions. The first soil horizon contains many significant components of the nutrient pool for coniferous forest structures (Prescott et al. 2000), therefore, retrieved soil samples were taken from this horizon.

The increase of litter and materials that fall into the soil as the forest structure changes increase the overall flux material input that goes into the soil matrix of components. This addition in the soil matrix increases the material that mineralizes while existing a decrease in the nutrient uptake of the roots, resulting in overall increased concentrations of the soil components (Rosén et al. 1996).

Nitrogen increases in its soil availability, more in its inorganic forms (Griffin et al. 2011; Cullings et al. 2003; Huber et al. 2004). These pools are prone to changes due to the increase in the carbon sources and soil humidity content, affecting processes such as nitrification, denitrification, and mineralization (Mikkelson et al. 2013).

If nitrification occurs and $NO_3$ concentrations increase, this negatively charged component may attract base cations such as aluminum ions (Huber et al. 2004), if this is the case, base cations should be expected to increase with the transition of the forest structure.

Several laboratory tests were conducted for the estimation of organic matter content, total nitrogen, total phosphorus, and exchangeable cations, along with measurements of humidity content, pH, and electrical conductivity. Tests were performed between February and June in the laboratory facilities of the University of Guadalajara. Analytical tests and measurements performed are described in the section below.

## Organic matter content:

Determination of organic matter was done by a modified method from the Walkley-Black method for soil organic carbon (Mylavarapu et al 2014). This method quantifies the organic matter content through wet chemical oxidation, oxidizing the organic matter of the sample. The method is done by treating the soil with potassium dichromate, sulfuric acid, distilled water, and phosphoric acid. The potassium dichromate that does not reacts is determined through titration with ferrous sulfate, which with a recovery factor the soil organic carbon content is quantified (Wang et al, 2012).

Sample preparation:

For each sample, 0.10 grams of dry sieved (1 mm) soil was prepared and added into an Erlenmeyer flask. Next, 5 mL of potassium dichromate ($K_2Cr_2O_7$) 1 N, afterward, 10 mL of sulfuric acid ($H_2SO_4$) were added, each sample was shaken and then left for 30 minutes for the reaction to finish. Each flask was filled with distilled water up to the 200 mL volume of the flask. 5 ml of phosphoric acid are added along with 0.5 mL of diphenylamine as an indicator. Each sample was titrated with ferrous sulfate ($FeSO_4$). Two reference solutions are also prepared to determine the ferrous sulfate normality.

After titration of each sample normality of the ferrous sulfate is calculated based on the titration average. For the two reference solutions. Equation 1 presented below estimates the normality of the ferrous sulfate.

$$N_{FeSO_4} = \frac{volume\ of\ K_2Cr_2O_7 * \ K_2Cr_2O_7\ normality}{titrated\ volume\ of\ FeSO_4}$$

*Equation 1. Normality of ferrous sulfate equation.*

After, the estimation of normality can be included in Equation 2 to calculate the organic matter content.

$$Organic\ matter\ content\ (\%) = \left[\frac{(volume\ of\ K_2Cr_2O_7 * K_2Cr_2O_7\ normality) - (titrated\ volume\ of\ FeSO_4 * FeSO_4\ normality)}{grams\ of\ soil\ sample}\right] * 0.69$$

*Equation 2. Organic matter equation.*

## Total nitrogen:

Nitrogen was quantified in the retrieved samples by a Kjeldahl technique for soils (Bremmer, 1965). 2 grams of previously sieved (2mm) soil was first digested and then distilled with a Kjeldahl apparatus. The soil was put into a Kjeldahl flask with a mix of copper sulfate and sodium sulfate and 30 mL of sulfuric acid, samples are heated for about an hour until they reach an emerald green precipitate. After cooling, samples were added 300 mL of distilled water, a spoon of zinc pearls, and 100 mL of NaOH, flasks are distilled within the apparatus, the distilled gas was received in a solution with 50 mL of boric acid at 4% and 5 drops of the indicator methyl red - bromocresol green.

Once the distillation surpassed 300 mL samples are titrated with HCL 0.1 N. With the titrated volume, equation 3 serves to calculate the total nitrogen percentage in the sample.

$$Total\ N\ (\%) = \frac{titrated\ volume\ (mL) * N * eq}{mass\ sample\ (g)} * 100$$

*Equation 3. Total nitrogen percentage.*

## Soil pH and Electric conductivity:

Soil pH and electric conductivity were measured for all soil samples. Preparation for the measurements was done by adding 20.00 grams of dry sieved (1.5 mm) soil into flasks and filled with 40 mL of distilled water. Subsequently, samples were put into an orbital shaker for 30 minutes. Electric conductivity was measured using a YSI model 35 conductance meter, while pH was measured with a Beckman pH meter Model Φ40.

## Phosphorus:

The quantification of phosphorus was done via the Bray P1 extract (Kurts, 1945). This technique is for soils with an acidic pH and serves as an index for available phosphorus in the soil, by removing the phosphorus complexes into an acidic solution with ammonium fluoride and hydrochloric acid.

Sample preparation:

Four solutions were prepared:

1. Extracting solution: contained 30 mL of $NH_4F$ 1 N, 50 mL HCl 0.5 N in a 1 L volumetric flask with distilled water.

2. molybdate sulfur solution: 40 g ammonium molybdite $(NH_4)_6Mo_7O_{24}*4H_2O$ in 500 mL distilled water. Dissolve 0.972g of antimuonium and potassium tartrate and add 492 mL of concentrated $H_2SO$ in a 2 L flask with distilled water.
3. Working solution: 60 mL of the molybdite sulfur in 800 mL of distilled water, dissolve 1.056 g of ascorbic acid, and dilute to one liter. The solution must be prepared each day samples are quantified.
4. Standard solution of phosphorus (100ppm): 0.4394 g of potassium phosphate ($KH_2PO_4$).

Two grams of previously dry and sieved soil (2mm) was added to 20 mL of the extracting solution and agitated at 180 rpm for 10 minutes and filtered with a Whatman # 2 filter. Afterward, 2 mL of this extract were transferred to a colorimetric tube, adding 8 mL of the working solution and waiting at least 10 minutes for the color formation. Intensity absorbance was measured in a spectrophotometer at 882 nm to be furtherly used in equation 4.

Calibration curve:

Based on the standard solution a calibration curve was created measuring the intensity of solutions while varying the ml of aliquot for the standard solution. Concentrations were obtained in parts per million through the linear equation (equation 4) found in the calibration curve.

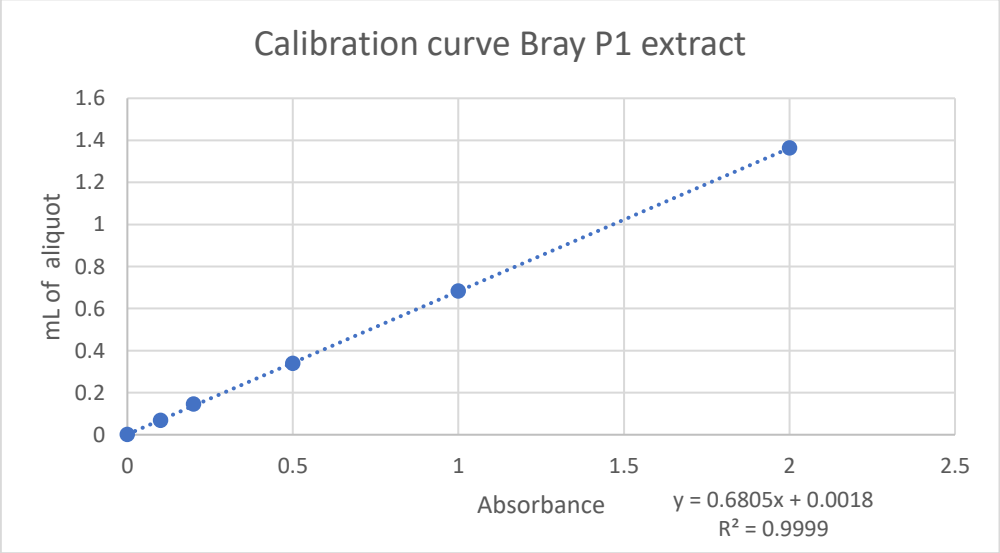


*Figure 4 Calibration curve for phosphorus concentrations*

$$phosphorus\ concentration\ (ppm) = (0.6805 * absorbance) + 0.0018$$

*Equation 4. phosphorus concentration.*

## Soil cation exchange capacity:

The technique for exchangeable cations (Thomas, 1982) was followed for the quantification of the soil cation exchange capacity. 5 grams dried and sieved soil

(3mm) were put in a small Erlenmeyer flask with 30mL of ammonium acetate, samples were agitated in an orbital agitator for 30 minutes at 180 rpm. Afterward, samples were filtrated with a Whatman # 2 filter.

Filtrated samples were analyzed with a Variant atomic absorption spectrophotometer, model 240 FS. Calcium was measured at 422.7 nm, magnesium at 285.2 nm while potassium and sodium were measured in the same equipment through flame emission. Concentrations were given by the variant equipment in mg/kg.

### Humidity:

10 grams of 2 mm sieved soil were dried in crucibels in a Felisa oven at 100 Celsius degrees for 24 hours and weighted with a Sartorius balance, humidity was calculated in percentage by the loss of weight from the original 10 grams

$$humidity\ content\ (\%) = (Humid\ weight - dry\ weight) * \frac{100}{humid\ weight}$$

*Equation 5. Humidity content (%).*

### Matrix construction:

To determine how much soil components changes are correlated at different altitudes and between forest structures a Pearson Correlation Coefficient (PCC) analysis and a Principal Component Analysis were performed to the soil components data.

Matrix columns were arranged by each parameter average for the different forest structures, the tiles for the columns represented the altitudinal zone at which the averages corresponded.

### R methodology and packages:

The PCC and PCA were performed using as input the created soil component matrix. The required and used libraries for computing these tests were factomineR, factoextra, and tidyverse.

## Chapter 2.

## Remote sensing for data creation, interpretation, and vulnerability projections:

### Vegetation transitions and climate and weather analysis:

Representing and observing a spatial area within time by using Geographical Information Systems serves as a powerful tool for spatial and temporal analysis of a region. The imagery was processed with the use of the software ArcMap using imagery files from the USGS Glovis site and all correspond to Landsat satellites imagery. All imagery files were taken from December to February, depending on the cloud cover of the image and the moment the satellite swept the area.

Field exploration in the high mountain and the marking of georeferenced points permitted the creation of spectral signatures for the different forest structures of interest. Observing these spectral signatures at the georeferenced sites through a false-color composite image enabled the creation of a high mountain classification based on the vegetation and alpine terrain. This false-color composite image is the result of a composite band operation that shows the near-infrared band from the satellites in the visible red band, this since vegetation reflects the infrared spectrum of light (earth observatory NASA).

The high mountain classification was performed under a Maximum Likelihood Classification operation using the false-color vegetation composite images as a layer. By using pixel colorations from the spectral signatures, three major categories in the upper mountain were classified; green vegetation, alpine terrain, and yellow and grey vegetation. A total of 17 maximum likelihood classifications maps were created for the studied area comprehended between 3300-4270 (Appendix 2). These maps allowed to differentiate in time the color change of the pines needles from green to yellow, red, and grey of sites where bark beetle has migrated in the region of interest and furtherly quantify these categories as changing areas in time. The creation of the maps required a total of 85 spectral signatures from different sites and locations in the mountain (39 from the sampling locations, table 1. And 46 from reference points, appendix 1).

All maximum likelihood classification maps layouts and false vegetation indexes were made on a 1:110,000 scale and are shown across the UTM 13N grid( Appendix 2). Maps from 1989 to 1999 correspond to Landsat 5 imagery, 2001 to 2013 maps correspond to Landsat 7 and lastly, maps from 2014 to 2020 correspond to Landsat 8 imagery. The designated colors for the maximum likelihood classification were green for the green vegetation category, grey for the alpine terrain, and yellow for the yellow and grey vegetation.

Radiometric corrections based on sun elevation were performed to correct the images. Selected images did not include any cloud cover. For Landsat 7 and 8 imagery, a panchromatic operation was performed for all these images which allowed to increase each pixel's resolution from 30x30m to 15x15m

### Altitudinal zones and classified areas:

Four altitudinal zones were selected to be studied and analyzed, the first zone ranges from 3300 masl to 3400 masl, the second zone covers the area between 3400 to 3600 masl, the third zone is 3600-3800 masl and lastly, the uppermost zone covers the areas between 3800 and 4270 masl. To create these altitudinal zones a Digital Elevation Model (DEM) was needed to create contour lines around these zones. The DEM used was from ASTER Earth data from NASA. Figure 5 shows the resulting altitudinal zones for the VCC, the image is shown in a UTM 13N grid, through a true color composite image.

Images from 1989 to 1999 correspond to Landsat 5 satellite imagery.

The resulting total area of the study (3300-4260 masl) is 4212 hectares. All areas estimations were based on the pixel count obtained by the maximum likelihood classifications. For Landsat 5 images each pixel count for the three categories was multiplied by the area of the pixel resolution (30m x 30m) and divided by 10,000 to convert to hectares. For Landsat 7 and 8 imagery, the multiplied resolution was 15m x 15m. All maximum likelihood classifications and false color compilations are included in appendix 2.

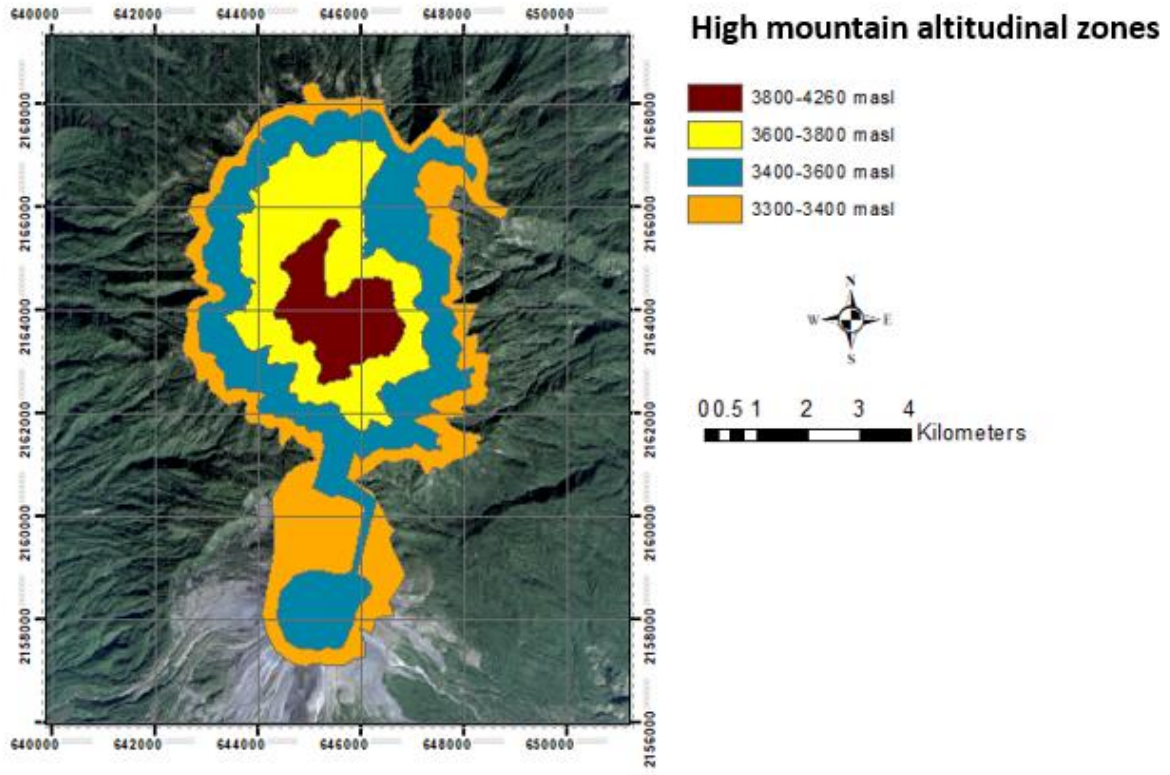


*Figure 5. Altitudinal zones for VCC.*

## Weather data:

The station found at the high mountain zone is part of the National Water Commission (CONAGUA), the station started to operate starting 2013, all historic data until 2020 was given by CONAGUA. The station takes measurements for each of the parameters every 10 minutes. All historic data was averaged the following way:

- Annual averages (appendix 1).
- Seasonal averages: made up of four quartiles per year.

Measured and processed parameters were air temperature, radiation, humidity, and precipitation, this last one was not averaged but was the total annual and seasonal cumulation of rain fall.

## Analysis of meteorological data and changes of vegetation for VCC:

To evaluate the vulnerability of the high mountain pine towards bark beetle migrations and outbreaks in response to weather conditions and climate change, two statistical tests were performed, Pearson Correlation Coefficient (PCC) and a Principal Component Analysis (PCA), both processes used the generated data from maximum likelihood maps and historical weather data. The weather parameters used to correlate the change in vegetated areas due to forest transitions were precipitation, relative humidity, air temperature, and radiation.

The VCC has seen recent bark beetle outbreaks (starting 2015 as seen in maximum likelihood classifications in appendix 2) that have resulted in big extensions of the high mountain transitioning from green vegetation to yellow, red, and grey vegetation. The increased outbreaks in the high altitudinal zones appear to be related to warmer periods in the mountain as well as a decrease in local humidity and the total annual precipitation. The PCC and PCA had the objective of determining and correlating how much of these bark beetle outbreaks and migrations are related to the climate and weather conditions.

Classification of variables consisted in selecting the changes of vegetation attributed to the bark beetle dynamic in the high mountain as dependent variables, and in using the processed weather data as independent variables for being possible drivers of this dynamic.

## Dependent variables:

Dependent variables were selected as the changes of vegetation perceived by the maximum likelihood classifications maps for the whole study area as well as the four selected altitudinal zones, these changes of vegetation were calculated based on the change of green vegetation area in hectares between each of the studied years. Positive values denote a decrease in green vegetation, that is area of sectors of pine that transitioned from green vegetation to yellow or grey vegetation, while negative values express an increase in green vegetation area, that is, restored areas that changed to green vegetation as a result from conservation and reforestation.

| **Dependent variables** | **Explanation** |
|---|---|
| Gross change of vegetation | Area of the mountain vegetation that changed from a green pine status to yellow or grey vegetation, expressed in hectares per analyzed periods in the whole study area (3300-4260masl) |
| % gross change of vegetation | Percentage of the mountain vegetation that changed from a green status to a yellow or grey status per period analyzed in terms of % of total vegetation in the whole study area (3300-4260 masl) |
| Gross change of vegetation 3300-3400 masl | Area of the altitudinal zone between 3300-3400 masl that changed from a green pine status to yellow or grey vegetation, expressed in hectares per analyzed periods. |
| Gross change of | Area of the altitudinal zone between 3300-3400 masl that changed from a green pine |

| | |
|---|---|
| vegetation 3400-3600 masl | status to yellow or grey vegetation, expressed in hectares per analyzed periods. |
| Gross change of vegetation 3600-3800 masl | Area of the altitudinal zone between 3300-3400 masl that changed from a green pine status to yellow or grey vegetation, expressed in hectares per analyzed periods. |
| Gross change of vegetation 3800-4260 masl | Area of the altitudinal zone between 3300-3400 masl that changed from a green pine status to yellow or grey vegetation, expressed in hectares per analyzed periods. |

*Table 2. Dependent variables*

## Independent variables:

Independent variables were selected based on the three main factors that are considered to be drivers for bark beetle outbreaks (Creeden et al. 2013). Certain changes in air temperature, relative humidity, precipitation, and radiation can induce a greater capacity for the beetle to adapt to the mountain seasons, cold-induced mortality for the beetle can decrease at warmer periods, and host local trees can be under stress due to drought conditions (Bentz et al. 1991; Logan and Bentz, 1999; Logan and Powell, 2001). Therefore, air temperature, relative humidity, precipitation, and radiation were selected as independent variables. Variables were constructed as annual averages and as seasonal averages. Seasonal averages consisted of the average of three months, having 4 quartiles of seasonal averages per year.

| **Independent variables** | **Explanation** |
|---|---|
| Air temperature | Air temperature is measured in degrees Celsius. |
| Relative humidity | The relative humidity is expressed in terms of the percentage of concentration of water vapor in the environment. |
| Precipitation | Precipitation is quantified in mm of rainfall. Data comes in annual and seasonal millimeters of rain fall |
| Radiation | Radiation averages are expressed in $W/m^2$ |

Table 2. Independent variables

## Matrix construction:

To correlate the annual changes of vegetation with the weather variables, annual averages and seasonal averages per year were created. Meteorological data was averaged annually and in quartiles, the first quartile belonging from January to march, the second from April to June, the third quartile from July to September, and the last quartile from October to December. All data was compiled and merged into R and set for further analysis of PCC and the PCA.

## R methodology and packages:

The PCC was computed by merging all data in a yearly format as a data frame, all columns corresponded to all the variables of the study (weather conditions and changes of vegetation) while the rows represented the year of the value in the

column. Seasonal variation was introduced as columns, of four quartiles per measured parameter per year.

The PCA was computed with weather conditions of the annual data rather than as seasonal variations in the year, this allowed to reduce the dimensions of the operations. FactomineR, factoextra, and tidyverse libraries were used for computing the operation and creating the graphs.

# Results:

## Chapter 1: Quantification of soil components

This section shows the main results of the parameters measured and quantified for the different sampling locations at the VCC. Results are presented as follows: The first section includes the summary for the general parameters quantification, secondly, main estimations of parameter quantification by altitudinal zone and forest structure for all measured parameters. And lastly the statistical analysis tests (PCC and PCA) for the parameters data.

## Components:

The following table contains the concentrations of the different components measured for the 39 samples. Forest structure 1 refers to green sites, structure 2 corresponds to yellow sites, structure 3 to red sites while structure 4 shows grey sites.

| Sample | Forest structure | Altitude (masl) | Organic matter content (%) | Total nitrogen (%) | Total phosphorus (ppm) | $K^+$ | $Na^+$ | $Ca^{2+}$ | $Mg^{2+}$ | Humidity content (%) | pH | CE | Soil temperature at site (°C ) |
|---|---|---|---|---|---|---|---|---|---|---|---|---|---|
| 1 | 2 | 3423 | 20.2 | 0.25 | 20 | 470 | 441 | 2409 | 479 | 25.3 | 3.9 | 0.15 | 16 |
| 2 | 2 | 3441 | 16.5 | 0.24 | 30 | 478 | 577 | 2640 | 434 | 13.2 | 5.2 | 0.08 | 15 |
| 3 | 3 | 3522 | 5.6 | 0.21 | 9 | 504 | 474 | 2189 | 430 | 16.8 | 4.6 | 0.13 | 8 |
| 4 | 4 | 3598 | 8.0 | 0.22 | 18 | 472 | 494 | 2164 | 430 | 13.9 | 4.2 | 0.10 | 8 |
| 5 | 1 | 3596 | 6.3 | 0.15 | 6 | 501 | 606 | 1575 | 259 | 16.0 | 4.5 | 0.06 | 23 |
| 6 | 4 | 3359 | 10.0 | 0.16 | 12 | 434 | 532 | 1778 | 357 | 15.2 | 4.8 | 0.12 | 15 |
| 7 | 2 | 3334 | 3.9 | 0.14 | 3 | 327 | 426 | 1227 | 244 | 17.5 | 5.8 | 0.05 | 12 |
| 8 | 2 | 3807 | 4.9 | 0.11 | 28 | 542 | 509 | 1029 | 211 | 15.2 | 4.4 | 0.07 | 14 |
| 9 | 2 | 3766 | 3.6 | 0.13 | 29 | 517 | 557 | 1288 | 276 | 24.0 | 4.8 | 0.09 | 14 |
| 10 | 1 | 3779 | 2.2 | 0.10 | 28 | 496 | 726 | 1980 | 274 | 11.1 | 4.5 | 0.06 | 22 |
| 11 | 4 | 3752 | 7.6 | 0.12 | 34 | 292 | 477 | 1304 | 260 | 20.2 | 3.9 | 0.10 | 16 |
| 12 | 4 | 3695 | 5.9 | 0.12 | 55 | 436 | 542 | 1226 | 266 | 16.6 | 3.9 | 0.09 | 16 |
| 13 | 1 | 3640 | 7.0 | 0.16 | 30 | 435 | 470 | 1356 | 228 | 14.6 | 4.1 | 0.09 | 18 |
| 14 | 4 | 3628 | 9.0 | 0.16 | 8 | 420 | 469 | 1460 | 296 | 17.5 | 4.5 | 0.06 | 13 |
| 15 | 1 | 3900 | 3.9 | 0.10 | 3 | 293 | 455 | 927 | 213 | 16.5 | 4.4 | 0.07 | 4 |
| 16 | 3 | 3851 | 5.6 | 0.17 | 29 | 478 | 783 | 1358 | 330 | 24.8 | 3.8 | 0.15 | 5 |
| 17 | 2 | 3845 | 6.6 | 0.09 | 16 | 306 | 460 | 1037 | 233 | 18.6 | 5.4 | 0.07 | 4 |
| 18 | 1 | 3776 | 4.6 | 0.12 | 10 | 354 | 477 | 1124 | 223 | 12.2 | 4.7 | 0.06 | 8 |
| 19 | 4 | 3763 | 6.3 | 0.14 | 35 | 384 | 542 | 1380 | 260 | 18.8 | 4.0 | 0.14 | 11 |

| | | | | | | | | | | | | | |
|---|---|---|---|---|---|---|---|---|---|---|---|---|---|
| 20 | 3 | 3722 | 6.3 | 0.14 | 17 | 486 | 510 | 1548 | 292 | 15.1 | 5.0 | 0.08 | 12 |
| 21 | 1 | 3625 | 12.7 | 0.19 | 6 | 615 | 592 | 2250 | 341 | 6.0 | 4.7 | 0.07 | 17 |
| 22 | 1 | 3765 | 13.4 | 0.14 | 8 | 650 | 741 | 1463 | 306 | 19.2 | 4.2 | 0.08 | 14 |
| 23 | 1 | 3760 | 4.6 | 0.11 | 9 | 329 | 495 | 1237 | 260 | 10.1 | 5.4 | 0.05 | 16 |
| 24 | 1 | 3847 | 8.3 | 0.16 | 13 | 480 | 571 | 1328 | 249 | 7.0 | 4.7 | 0.05 | 22 |
| 25 | 1 | 3873 | 9.3 | 0.16 | 7 | 398 | 589 | 1412 | 298 | 9.0 | 4.1 | 0.07 | 13 |
| 26 | 4 | 3464 | 3.6 | 0.11 | 27 | 286 | 458 | 1201 | 235 | 10.8 | 5.2 | 0.06 | 7 |
| 27 | 4 | 3460 | 13.4 | 0.20 | 38 | 299 | 416 | 2092 | 306 | 7.8 | 5.2 | 0.05 | 8 |
| 28 | 4 | 3470 | 9.7 | 0.14 | 28 | 319 | 491 | 1457 | 287 | 9.8 | 5.3 | 0.05 | 18 |
| 29 | 1 | 3888 | 4.6 | 0.12 | 23 | 352 | 481 | 1152 | 246 | 15.3 | 4.4 | 0.06 | 16 |
| 30 | 1 | 3831 | 5.9 | 0.09 | 20 | 329 | 440 | 1064 | 231 | 5.4 | 5.2 | 0.06 | 7 |
| 31 | 2 | 3775 | 6.3 | 0.10 | 29 | 388 | 486 | 1266 | 277 | 14.2 | 4.1 | 0.07 | 6 |
| 32 | 1 | 3739 | 7.3 | 0.16 | 31 | 397 | 481 | 1253 | 272 | 12.8 | 3.9 | 0.07 | 6 |
| 33 | 4 | 3665 | 11.0 | 0.14 | 37 | 415 | 522 | 1822 | 392 | 15.5 | 3.7 | 0.09 | 8 |
| 34 | 2 | 3545 | 12.7 | 0.21 | 24 | 572 | 481 | 2365 | 409 | 16.2 | 4.2 | 0.10 | 6 |
| 35 | 1 | 3846 | 4.2 | 0.12 | 33 | 366 | 440 | 1225 | 260 | 15.8 | 5.2 | 0.06 | 8 |
| 36 | 4 | 3862 | 5.3 | 0.16 | 35 | 423 | 400 | 1604 | 361 | 22.2 | 3.6 | 0.13 | 7 |
| 37 | 4 | 3472 | 8.7 | 0.28 | 4 | 679 | 510 | 2478 | 433 | 9.4 | 5.1 | 0.11 | 8 |
| 38 | 1 | 3471 | 14.8 | 0.27 | 5 | 474 | 493 | 1328 | 303 | 12.0 | 4.7 | 0.07 | 8 |
| 39 | 4 | 3441 | 14.8 | 0.15 | 34 | 490 | 518 | 1845 | 385 | 14.9 | 4.0 | 0.08 | 8 |

*Table 3. Component's concentrations and sites.*

Detailed information for components status at different altitudes and forest structures is shown below. Tables show averages compiled by the forest structure of the site of the sample and by altitudes.

## Organic matter content:

| Organic matter | | | |
|---|---|---|---|
| **Altitudinal zone** | **Green structure** | **Yellow and red structure** | **Grey structure** |
| All zones | 6.8 | 8.8 | 8.7 |
| Zones 1 & 2 | 10.5 | 11.8 | 10.8 |
| Zone 3 | 6.4 | 7.4 | 8.0 |
| Zone 4 | 6.1 | 5.7 | 4.4 |

*Table 4. Organic matter content average by altitudinal zone and forest structure.*

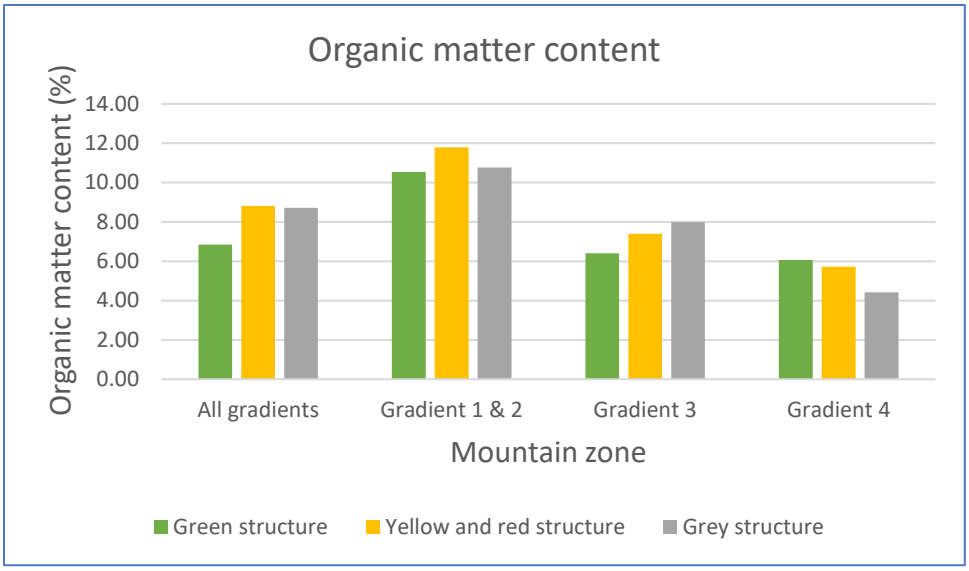


*Figure 6. Organic matter content by altitudinal zone and forest structure.*

There is an overall increase in organic matter content in the soil in sites that had the presence of migration. Zone 1 & 2 areas (3300-3600 masl had the highest concentrations. Only for the last zone, the organic matter content was greater in sites where outbreaks and migrations have happened.

## Nitrogen:

| Total nitrogen (%) | | | |
|---|---|---|---|
| **Altitudinal zone** | **Green structure** | **Yellow and red structure** | **Grey structure** |
| All zones | 0.14 | 0.16 | 0.16 |
| Zones 1 & 2 | 0.21 | 0.21 | 0.19 |
| Zone 3 | 0.14 | 0.13 | 0.14 |
| Zone 4 | 0.13 | 0.12 | 0.13 |

*Table 5. Total nitrogen average by altitudinal zone and forest structure.*

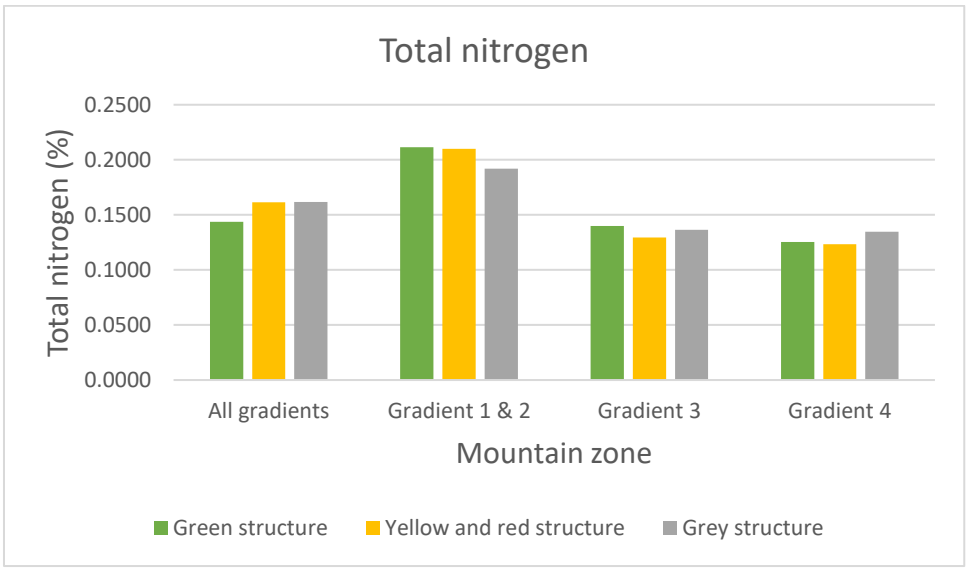

*Figure 7. Nitrogen interpretation for altitudinal zone and forest structure.*

There was an overall increase of the nitrogen in average by phases, but analyzing by zone the trend was not the same. For the region between 3300-3600 masl concentrations slightly decreased when moving to a grey structure, for zone 3 a slight decrease is seen in yellow and red structures, and then an increase is observed for the grey structures. The upper zone concentrations were similar for the first phases and the grey phase had an increase.

## Phosphorus:

| Phosphorus concentration (ppm) | | | |
|---|---|---|---|
| **Altitudinal zone** | **Green structure** | **Yellow and red structure** | **Grey structure** |
| All zones | 16 | 20 | 28 |
| Zones 1 & 2 | 5 | 17 | 22 |
| Zone 3 | 19 | 21 | 34 |
| Zone 4 | 17 | 24 | 31 |

*Table 6. Total phosphorus average by altitudinal zone and forest structure.*

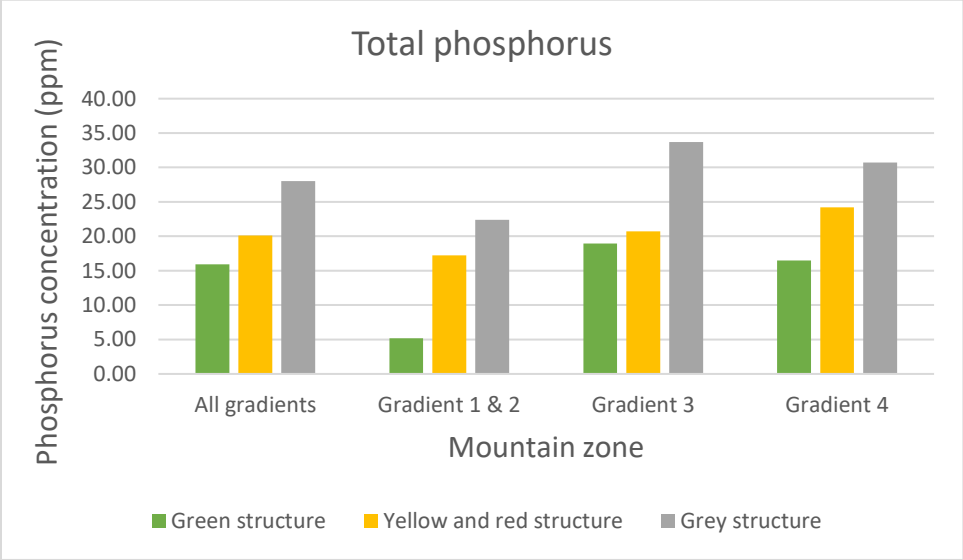


*Figure 8. Total phosphorus by altitudinal zone and forest structure.*

Phosphorus had an overall increase within all the studied zones and in general average. Each transition of a forest structure green-yellow & red-grey had a subsequent increase for all zones. The steepest change was in the first two zones, as the average concentration between a green forest structure and yellow and red structures was increased by 12 ppm. Zone 3 grey structure had the highest average concentration of phosphorus between all the zones and structures.

## Soil cation exchange capacity:

$K^+$

| $K^+$ concentration (mg/kg) | | | |
|---|---|---|---|
| **Altitudinal zone** | **Green structure** | **Yellow and red structure** | **Grey structure** |
| All zones | 416 | 476 | 411 |
| Zones 1 & 2 | 487 | 470 | 449 |
| Zone 3 | 438 | 510 | 389 |
| Zone 4 | 370 | 442 | 355 |

*Table 7: $K^+$ average concentrations by altitudinal zone and forest structure.*

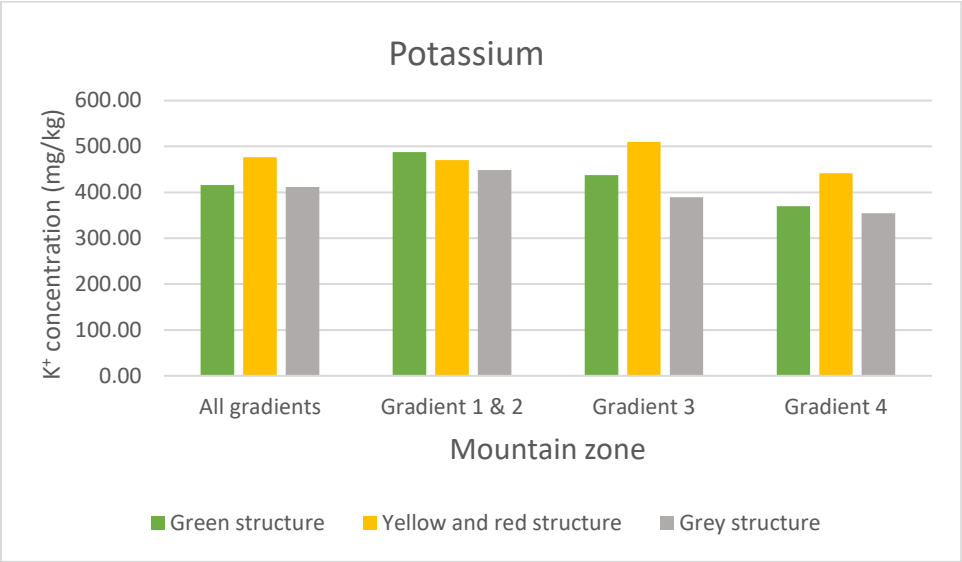


*Figure 9. $K^+$ average concentrations by altitudinal zone and forest structure.*

Overall, potassium concentration increased for the yellow and red forest structures but decreased within all of the grey structures at all zones. For the first two zones, the observed trend is that potassium decreased through each forest transition, as the average concentration for the green structures was above the yellow and grey structure. The upper zones of the mountain follow the overall trend, potassium concentration increases when transitioning to yellow and red structures and then decreased to concentrations lower than the green structures when reaching the grey transition.

$Na^+$

| $Na^+$ concentration (mg/kg) | | | |
|---|---|---|---|
| **Altitudinal zone** | **Green structure** | **Yellow and red structure** | **Grey structure** |
| All zones | 523 | 537 | 490 |
| Zones 1 & 2 | 550 | 480 | 493 |
| Zone 3 | 540 | 573 | 510 |
| Zone 4 | 496 | 584 | 429 |

*Table 8. $Na^+$ average concentrations by altitudinal zone and forest structure.*

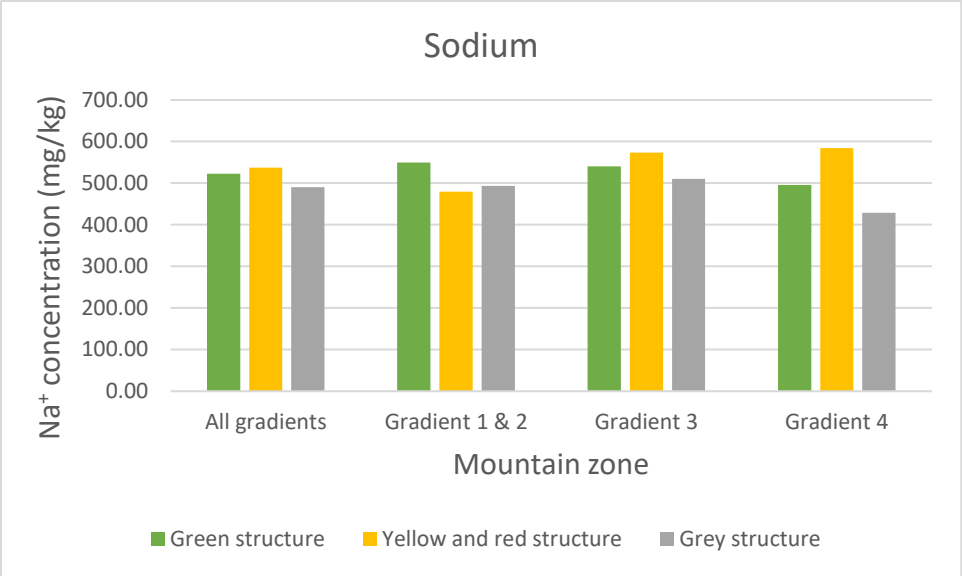


*Figure 10. $Na^{+}$ average concentrations by altitudinal zone and forest structure.*

Sodium had a similar trend as potassium, overall, the highest average concentration is found in yellow and red structures, and the lowest corresponded to the grey sites. Again, the upper zones increased when transitioning to yellow structures, followed by a decrease for the grey structures. Green forest structures for zones 1 and 2 had higher sodium ion concentrations than the other structures.

$Ca^{+2}$

| **$Ca^{+2}$ concentration (mg/kg)** | | | |
|---|---|---|---|
| **Altitudinal zone** | **Green structure** | **Yellow and red structure** | **Grey structure** |
| All zones | 1372 | 1651 | 1678 |
| Zones 1 & 2 | 1452 | 2166 | 1969 |
| Zone 3 | 1533 | 1391 | 1438 |
| Zone 4 | 1185 | 1141 | 1402 |

*Table 9. $Ca^{+2}$ average concentrations by altitudinal zone and forest structure.*

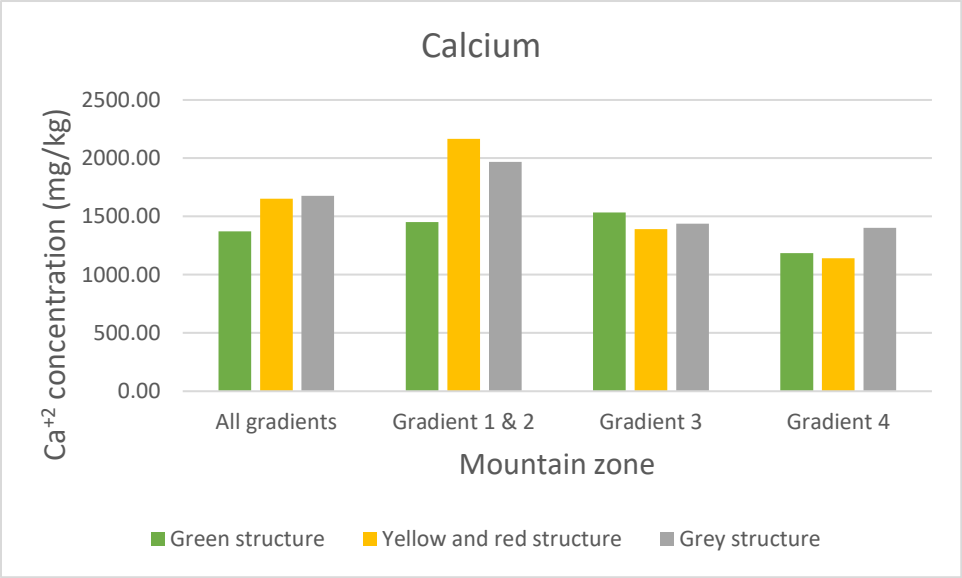


*Figure 11. $Ca^{+2}$ average concentrations by altitudinal zone and forest structure.*

Overall, calcium concentration increased through each transition, increasing by 300 mg/kg in the grey structure compared to the green sites. When analyzing zones behavior, yellow and red structures had the max concentration for the first zones

$Mg^{+2}$

| **$Mg^{+2}$ concentration (mg/kg)** | | | |
|---|---|---|---|
| **Altitudinal zone** | **Green structure** | **Yellow and red structure** | **Grey structure** |
| All zones | 261 | 327 | 328 |
| Zones 1 & 2 | 281 | 399 | 366 |
| Zone 3 | 266 | 288 | 295 |
| Zone 4 | 249 | 258 | 298 |

*Table 10. $Mg^{+2}$ average concentrations by altitudinal zone and forest structure.*

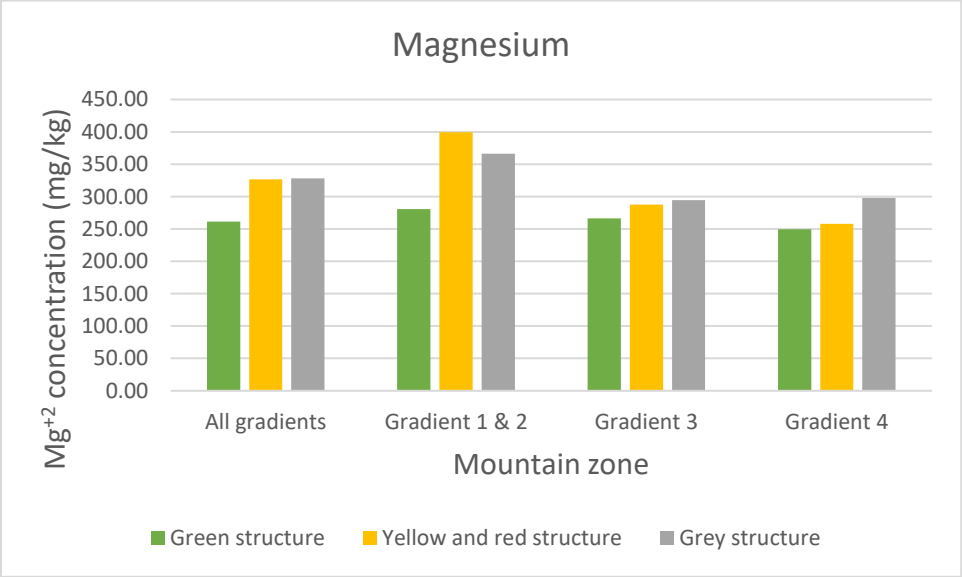


*Figure 12. $Mg^{+2}$ average concentrations by altitudinal zone and forest structure.*

Magnesium average concentrations increased overall through each forest transition, grey structure overall was 1.43 mg/kg higher than the yellow and red structures and approximately 65 mg/kg higher than the green structures. Zones 1 and 2 had the highest increase at the yellow and red structure, but for the upper most zones the grey structure was higher, increasing in concentration about 40 and 50 mg/kg concerning green and yellow structures respectively.

## Humidity:

| Humidity content (%) | | | |
|---|---|---|---|
| **Altitudinal zone** | **Green structure** | **Yellow and red structure** | **Grey structure** |
| All zones | 11.7 | 18.3 | 14.8 |
| Zones 1 & 2 | 14.0 | 17.8 | 11.8 |
| Zone 3 | 11.1 | 18.1 | 17.7 |
| Zone 4 | 11.5 | 19.5 | 16.5 |

*Table 11. Humidity content average by altitudinal zone and forest structure*

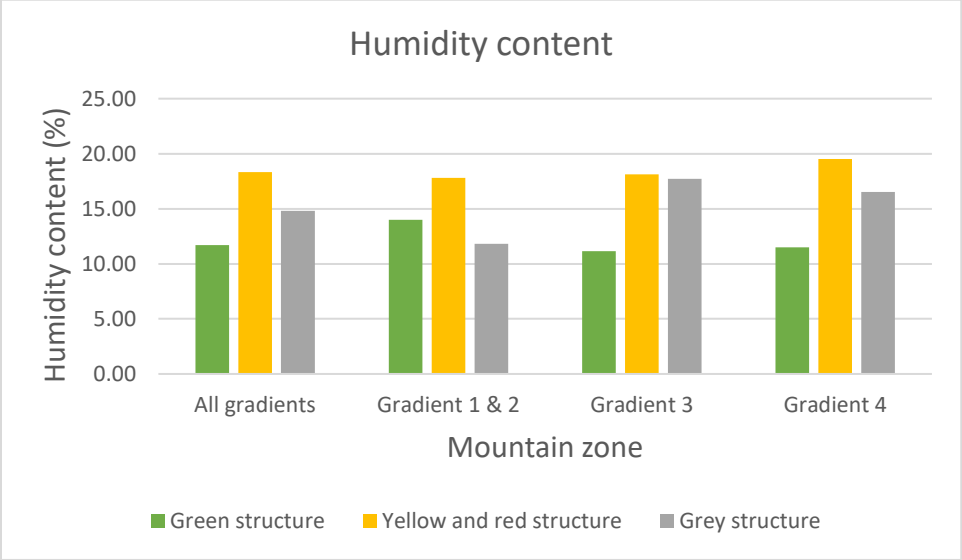


*Figure 13. Humidity content by altitudinal zone and forest structure.*

Humidity content saw an increase within all zones when changing from a green structure to a yellow or red one, and a small decrease when changing to a grey structure, though with greater content than the green structure. This trend was the same for all the analyzed structures and zones.

## pH:

| pH | | | |
|---|---|---|---|
| **Altitudinal zone** | **Green structure** | **Yellow and red structure** | **Grey structure** |
| All zones | 4.60 | 4.62 | 4.42 |
| Zones 1 & 2 | 4.61 | 4.73 | 4.76 |
| Zone 3 | 4.54 | 4.55 | 4.00 |
| Zone 4 | 4.66 | 4.52 | 4.44 |

*Table 12. pH average by altitudinal zone and forest structure.*

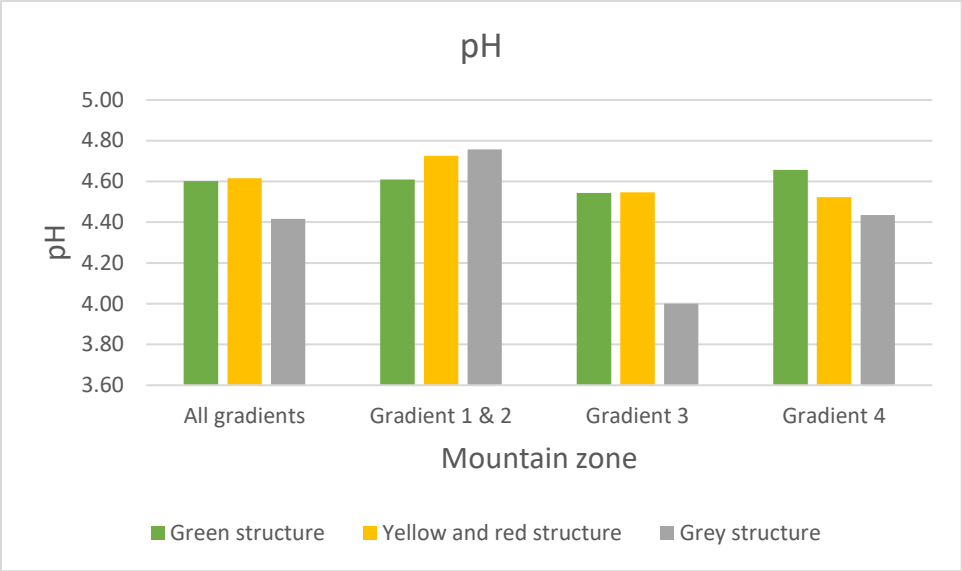


*Figure 14. pH by altitudinal zone and forest structure.*

The general trend of pH is that overall it became more acidic when transitioning to the grey structure, but when analyzing by zone there were two cases; the lower zones (3300-3600masl) had an increase of pH when transitioning through forest structures, while the upper zone had a decrease in pH with the same transition, being more noticeable for the grey phases sites of these zones.

## Chapter 2: High mountain vulnerability

### Classified Areas:

These are the resulting areas given by the pixel count of ArcMap for each of the maximum likelihood classifications in the period 1989-2020.

Table 9 shows the high mountain classified areas (green vegetation, yellow or grey vegetation, and alpine terrain) obtained by the maximum likelihood operation from each of the studied periods(1989-2020).

| **High mountain terrain classification total areas (ha)** | | | |
|---|---|---|---|
| Year | Green vegetation | Yellow and grey vegetation | Alpine terrain |
| 1989 | 2061 | 1536 | 615 |
| 1993 | 1907 | 1732 | 572 |
| 1995 | 1901 | 1736 | 574 |
| 1999 | 1885 | 1787 | 539 |
| 2001 | 1925 | 1757 | 530 |
| 2003 | 1852 | 1871 | 490 |
| 2005 | 2118 | 1584 | 511 |
| 2008 | 2322 | 1321 | 570 |
| 2010 | 2529 | 1169 | 515 |
| 2013 | 2445 | 1281 | 488 |
| 2014 | 2511 | 1178 | 523 |
| 2015 | 2698 | 953 | 562 |
| 2016 | 2495 | 1152 | 564 |
| 2017 | 2445 | 1275 | 493 |
| 2018 | 2291 | 1437 | 484 |
| 2019 | 2001 | 1741 | 471 |
| 2020 | 2061 | 1634 | 518 |

*Table 13. Region of study classified areas by forest and mountain structure*

Table 13 shows the gross change of vegetation in all of the studied areas, which denotes hectares of forest that have transitioned from a green structure to a yellow or grey structure (positive value in table) and vice versa(negative value in table) based on the difference of annual areas for each the studied periods.

| **Gross change of vegetation** | | |
|---|---|---|
| Year | Gross change of vegetation (ha) | Percentage gross change of vegetation (%) |
| 1993 | 154 | 4.2 |
| 1995 | 6 | 0.2 |
| 1999 | 16 | 0.4 |

| | | |
|---|---|---|
| 2001 | -40 | -1.1 |
| 2003 | 73 | 2.0 |
| 2005 | -266 | -7.2 |
| 2008 | -204 | -5.6 |
| 2010 | -207 | -5.6 |
| 2013 | 84 | 2.3 |
| 2014 | -66 | -1.8 |
| 2015 | -187 | -5.1 |
| 2016 | 203 | 5.6 |
| 2017 | 50 | 1.3 |
| 2018 | 154 | 4.1 |
| 2019 | 290 | 7.7 |
| 2020 | -60 | -1.6 |

*Table 14. Gross change of vegetation in all the studied area*

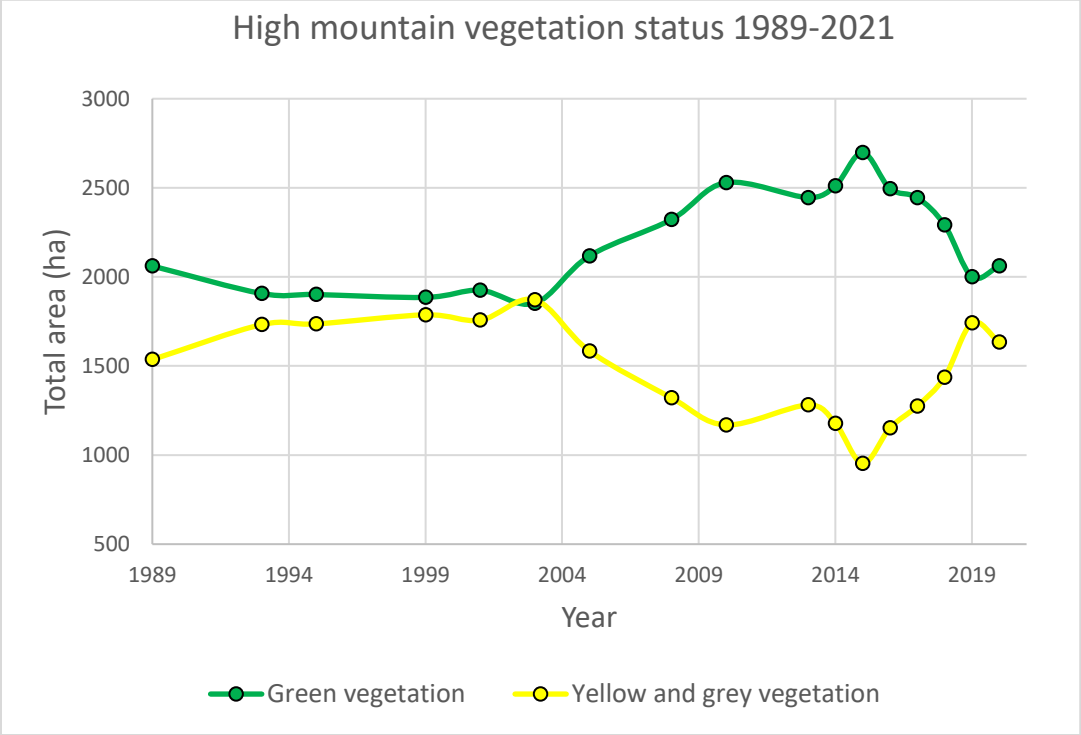


*Figure 15. High mountain vegetation status 1989-2020*

Forests structures are in constant transition as can be seen from the overall gross change of vegetation, where certain periods appear to have restoration of the grey structure to green structure and certain periods show the opposite transition. Between 2005 and 2010 an overall transition of forest regeneration towards a green structure is observed, where 777 hectares of the mountain transitioned from a grey structure to a green one. Starting 2016 a contrary trend can be observed, as 697 hectares transitioned from a green forest structure to a yellow or grey structure. 2005 and 2019 are the years with the greatest transition in areas with changes of -7.2% of the total vegetated area and 7.7% respectively.

Table 15 shows the classified areas of each of the maximum likelihood maps by altitudinal zone, while table 16 denotes the gross change of vegetation in each of those zones based on each period's change of vegetated area.

| Altitudinal zone areas (ha) | | | | | | | | | | | | |
|---|---|---|---|---|---|---|---|---|---|---|---|---|
| Year | Green vegetation | | | | Yellow and grey vegetation | | | | Alpine terrain | | | |
| | 3300-3400 masl | 3400-3600 masl | 3600-3800 masl | 3800-4260 masl | 3300-3400 masl | 3400-3600 masl | 3600-3800 masl | 3800-4260 masl | 3300-3400 masl | 3400-3600 masl | 3600-3800 masl | 3800-4260 masl |
| 1989 | 950 | 737 | 302 | 72 | 189 | 553 | 652 | 142 | 179 | 224 | 27 | 185 |
| 1993 | 937 | 717 | 197 | 56 | 214 | 578 | 757 | 183 | 166 | 219 | 28 | 159 |
| 1995 | 947 | 682 | 210 | 62 | 198 | 611 | 754 | 173 | 173 | 219 | 19 | 163 |
| 1999 | 879 | 693 | 244 | 69 | 259 | 603 | 734 | 191 | 179 | 217 | 4 | 139 |
| 2001 | 946 | 654 | 258 | 67 | 201 | 644 | 720 | 192 | 172 | 216 | 5 | 137 |
| 2003 | 910 | 717 | 170 | 55 | 255 | 613 | 780 | 223 | 155 | 214 | 2 | 119 |
| 2005 | 915 | 817 | 313 | 73 | 214 | 483 | 668 | 219 | 191 | 214 | 1 | 105 |
| 2008 | 943 | 895 | 396 | 88 | 182 | 401 | 571 | 167 | 194 | 219 | 15 | 142 |
| 2010 | 986 | 983 | 458 | 102 | 148 | 315 | 518 | 188 | 186 | 216 | 6 | 107 |
| 2013 | 1000 | 999 | 362 | 84 | 138 | 301 | 616 | 226 | 183 | 214 | 4 | 87 |
| 2014 | 972 | 993 | 458 | 88 | 167 | 304 | 513 | 194 | 181 | 217 | 10 | 115 |
| 2015 | 999 | 1079 | 521 | 99 | 125 | 218 | 435 | 175 | 196 | 217 | 27 | 122 |
| 2016 | 982 | 992 | 424 | 97 | 128 | 299 | 541 | 184 | 209 | 222 | 17 | 116 |
| 2017 | 880 | 904 | 523 | 138 | 245 | 397 | 457 | 176 | 194 | 214 | 2 | 83 |
| 2018 | 973 | 865 | 362 | 91 | 169 | 434 | 616 | 218 | 177 | 215 | 4 | 88 |
| 2019 | 914 | 742 | 271 | 74 | 231 | 558 | 710 | 242 | 175 | 214 | 1 | 81 |
| 2020 | 939 | 775 | 272 | 75 | 201 | 524 | 695 | 214 | 180 | 216 | 14 | 108 |

*Table 15. Classified areas by forest and mountain structure.*

| Gross changes of vegetation by altitudinal zones (ha) | | | | |
|---|---|---|---|---|
| Year | 3300-3400 masl | 3400-3600 masl | 3600-3800 masl | 3800-4260 masl |
| 1993 | 13 | 20 | 105 | 16 |
| 1995 | -10 | 35 | -13 | -6 |
| 1999 | 68 | -11 | -34 | -7 |
| 2001 | -67 | 39 | -14 | 2 |
| 2003 | 36 | -63 | 88 | 12 |
| 2005 | -5 | -100 | -143 | -18 |
| 2008 | -28 | -78 | -83 | -15 |
| 2010 | -43 | -88 | -62 | -14 |
| 2013 | -14 | -16 | 96 | 18 |
| 2014 | 28 | 6 | -96 | -4 |
| 2015 | -27 | -86 | -63 | -11 |
| 2016 | 17 | 87 | 97 | 2 |
| 2017 | 102 | 88 | -99 | -41 |
| 2018 | -93 | 39 | 161 | 47 |
| 2019 | 59 | 123 | 91 | 17 |
| 2020 | -25 | -33 | -1 | -1 |

*Table 16. Gross change of vegetation by altitudinal zones.*

## Altitudinal zones area coverage:

Figure 16 below shows a comparison of green vegetated areas with yellow and grey vegetated areas for each of the four altitudinal zones for the 1989-2020 period.

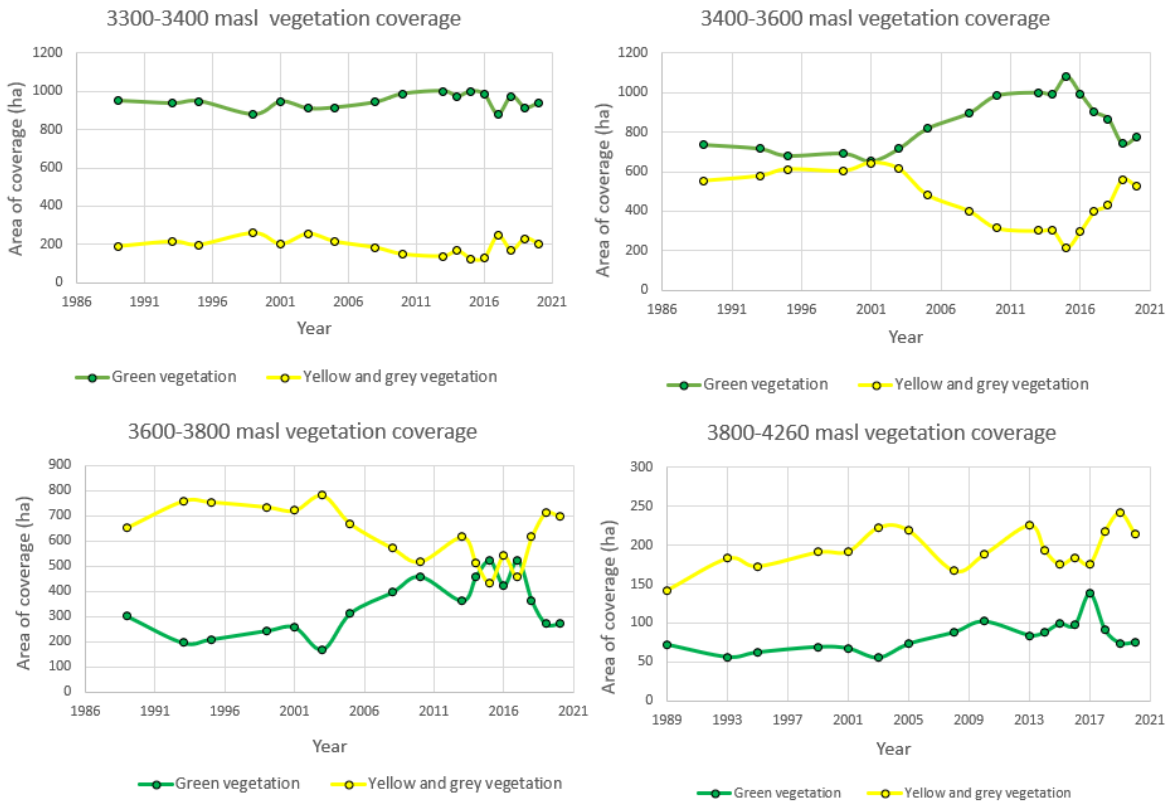


*Figure 16. High mountain vegetation status by altitudinal zones.*

The greatest change in vegetation due to bark beetle sprouts is between 3400 and 3800, with a decrease of 404 hectares of green vegetation to grey vegetation between 2014 and 2021, representing a decrease of 16.19 percent of the whole zone area. Though not as significant a recent decrease is also seen in the highest zone, where it has decreased by 27 hectares in the last decade, it represents 6.77 percent of the entire upper zone area. Vegetation coverage within the first zone (3300-3400masl) has maintained a constant status between both vegetations coverages, though in 2017 a relatively steep decline is observed for the green structure. The high elevation forest within this zone is composed of *Pinus Hartwegii* and *Abies Religiosa.*

## Weather data processing:

Tables 17 & 18 show the annual and seasonal compilation respectively of the processed weather data (2013-2020) and the variables used. Precipitation shows the

rain cumulation while relative humidity, air temperature, and radiation are shown as averages.

| Annual values | | | | |
|---|---|---|---|---|
| Year | Precipitation (mm) | Average relative humidity (%) | Average air temperature (°C) | Average radiation (W/m$^2$) |
| 2013 | 1727.0 | 67.2 | 8.7 | 199.6 |
| 2014 | 1302.2 | 70.5 | 8.4 | 179.2 |
| 2015 | 1760.4 | 73.0 | 8.5 | 177.7 |
| 2016 | 1323.4 | 64.7 | 8.7 | 158.3 |
| 2017 | 1222.2 | 64.2 | 8.9 | 305.6 |
| 2018 | 1241.4 | 72.4 | 8.4 | 195.4 |
| 2019 | 998.0 | 67.7 | 9.1 | 213.8 |
| 2020 | 1195.0 | 68.7 | 9.1 | 219.3 |

*Table 17. Annual values of the weather parameters.*

Seasonal averages are shown as quartiles, each quartile represents 3 months. Quartile 1 is the average of the data comprehended from January to March, Quartile 2 April-June, Quartile 3 July-September, and Quartile 4 October- December.

| Quartile | 2013 | | | | 2014 | | | |
|---|---|---|---|---|---|---|---|---|
| | AT | RH | Precipitation | Radiation | AT | RH | Precipitation | Radiation |
| 1 | 7.6 | 49.1 | 44.8 | 212.8 | 7.5 | 49.6 | 10.2 | 225.4 |
| 2 | 11.0 | 53.3 | 221.0 | 257.0 | 9.9 | 69.0 | 368.4 | 161.2 |
| 3 | 8.6 | 90.3 | 1188.4 | 166.5 | 8.9 | 91.3 | 646.2 | 156.5 |
| 4 | 7.6 | 76.2 | 272.8 | 162.0 | 7.5 | 71.9 | 277.4 | 173.5 |
| **Quartile** | **2015** | | | | **2016** | | | |
| | **AT** | **RH** | **Precipitation** | **Radiation** | **AT** | **RH** | **Precipitation** | **Radiation** |
| 1 | 6.4 | 62.2 | 477.4 | 191.7 | 7.4 | 36.8 | 45.0 | 242.4 |
| 2 | 9.9 | 71.1 | 197.4 | 174.6 | 10.8 | 57.3 | 194.8 | 218.8 |
| 3 | 8.9 | 86.5 | 420.0 | 170.8 | 8.8 | 88.8 | 829.2 | 88.9 |
| 4 | 8.7 | 72.1 | 665.6 | 173.6 | 7.7 | 76.1 | 254.4 | 83.3 |
| **Quartile** | **2017** | | | | **2018** | | | |
| | **AT** | **RH** | **Precipitation** | **Radiation** | **AT** | **RH** | **Precipitation** | **Radiation** |
| 1 | 7.4 | 49.1 | 44.8 | 221.0 | 7.3 | 59.4 | 61.0 | 210.5 |
| 2 | 11.4 | 50.5 | 167.4 | 259.1 | 10.3 | 68.3 | 228.4 | 232.2 |
| 3 | 8.9 | 90.4 | 911.6 | 170.5 | 8.6 | 92.1 | 471.8 | 172.2 |
| 4 | 7.9 | 66.9 | 98.4 | 204.2 | 7.4 | 69.7 | 480.2 | 166.8 |
| **Quartile** | **2019** | | | | **2020** | | | |
| | **AT** | **RH** | **Precipitation** | **Radiation** | **AT** | **RH** | **Precipitation** | **Radiation** |
| 1 | 8.6 | 47.3 | 15.0 | 242.6 | 8.1 | 58.0 | 238.6 | 212.0 |
| 2 | 11.2 | 52.4 | 91.0 | 265.1 | 11.1 | 59.3 | 225.6 | 264.3 |
| 3 | 8.9 | 91.6 | 639.4 | 175.3 | 9.0 | 93.5 | 701.4 | 182.0 |
| 4 | 7.8 | 79.6 | 252.6 | 172.3 | 8.3 | 63.9 | 29.4 | 218.7 |

*Table 18. Quartile annual averages for weather parameters.*

The following figures show grouped parameters and their seasonal and annual variation for the period 2013-2020. Figures 17 & 18 show annual variation of average air temperature and radiation, and precipitation and relative humidity respectively.

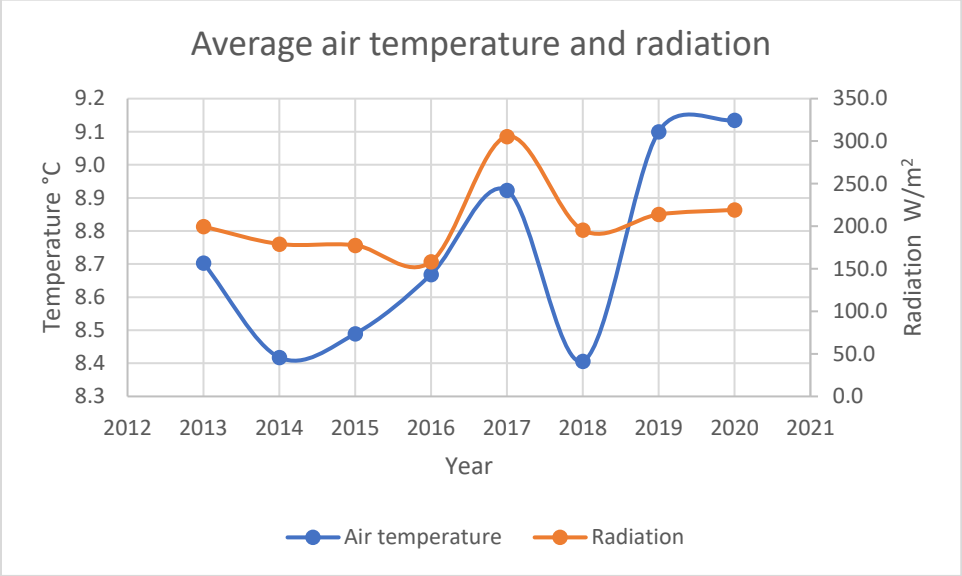


*Figure 17. Air temperature and radiation annual averages 2013-2020*

An overall increase in the average values for air temperature and radiation is observed in the 8-year data with respect 2013. Both parameters show similar trends. 2017 and 2019 have the steepest increase for an increase in average temperature, air temperature continued to increase in the overall average through 2020.

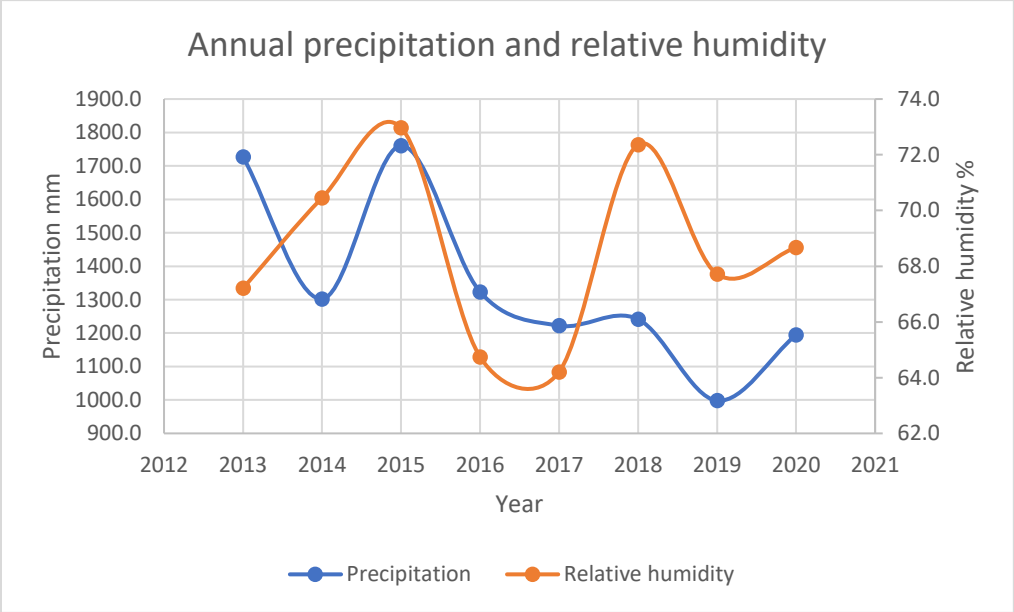


*Figure 18. Annual precipitation and average relative humidity for the period 2013-2020*

Annual precipitation and relative humidity show similar trends between 2014 and 2020, but changes in relative humidity had a steeper change concerning the annual averages than precipitation. The overall annual precipitation decreased and had a

historic lowest for the data in 2019, being the only year with less than 1000 mm of precipitation.

Figure 19 shows the seasonal comparison for the weather parameters period 2013-2020.

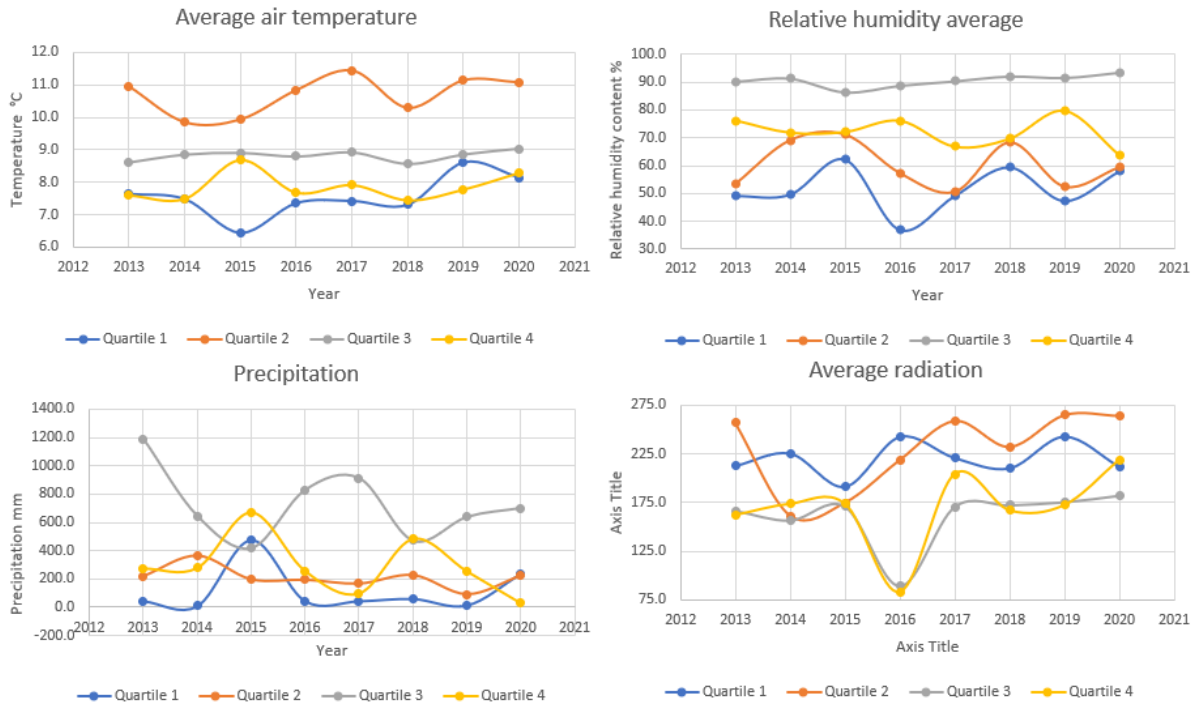


*Figure 19. Weather parameters annual comparison by quartiles*

Weather parameters observed as seasonal variations had a constant fluctuation in the studied period (2013-2020). Air temperature averages for each quartile had an overall increase in the whole studied period with a more significant increase in quartiles 2, 3, and 4. Radiation shows also an overall increase in averages values for quartiles 2, 3, and 4, being the most significant quartile 4. Precipitation had a constant variation for each season through the years, but the most significant changes are found in quartiles 3 and 4 where an overall decrease in rainfall is observed. Relative humidity hand and average increase for quartiles 1, 2, and 3, and an overall decrease for quartile 4.

## Pearson Correlation Coefficient:

A PCC was conducted between the vegetation both in the region of study and at the different altitude zones and the annual and seasonal weather parameters. Tables 19-23 show the results of the PCC. All values for this test are found between -1 and 1, a greater absolute value indicates a stronger correlation between the compared variables.

Table 19 shows the results for the correlation between the seasonal weather parameters and the gross change of vegetation in all of the studied areas. Tables 20-23 represent the correlation comparison of altitudinal changes of vegetation and its correlation with annual and seasonal precipitation, relative humidity, air temperature, and radiation respectively.

## Gross change of vegetation in the whole study area correlation between variables

| Gross Change of Vegetation (3300-4260 masl) | Annual Average correlation | Q1 | Q2 | Q3 | Q4 |
|---|---|---|---|---|---|
| Precipitation | -0.5530 | -0.7249 | -0.5349 | 0.2509 | -0.2433 |
| Relative humidity | -0.4812 | -0.6137 | -0.5757 | 0.2906 | 0.5631 |
| Air temperature | 0.3201 | 0.5841 | 0.5117 | -0.4382 | -0.6328 |
| Radiation | 0.1535 | 0.7720 | 0.5548 | -0.3141 | -0.4509 |

*Table 19. PCC of Gross changes of vegetation in the altitudinal zones and weather variables.*

## Changes of vegetation by altitudinal zone and its correlation with weather parameters

| Change of vegetation due to precipitation through Pearson correlation coefficient | | | | | |
|---|---|---|---|---|---|
| Altitudinal zone | Annual variation | Q1 | Q2 | Q3 | Q4 |
| 1 | 0.3425 | -0.3558 | -0.2837 | 0.3801 | -0.5207 |
| 2 | -0.7361 | -0.7647 | -0.4668 | 0.1943 | -0.4078 |
| 3 | -0.1265 | -0.3273 | -0.3429 | 0.0807 | 0.1306 |
| 4 | -0.0674 | -0.2242 | 0.0143 | -0.1983 | 0.3309 |

*Table 20. PCC of changes of vegetation in the altitudinal zones due to precipitation.*

| Change of vegetation due to relative humidity through Pearson correlation coefficient | | | | | |
|---|---|---|---|---|---|
| Altitudinal zone | Annual variation | Q1 | Q2 | Q3 | Q4 |
| 1 | -0.7097 | -0.5714 | -0.6334 | -0.0744 | 0.1598 |
| 2 | -0.6317 | -0.6871 | -0.6083 | 0.2678 | 0.3605 |
| 3 | 0.0010 | -0.1743 | -0.1590 | 0.2253 | 0.4441 |
| 4 | 0.4387 | 0.1454 | 0.2455 | 0.3324 | 0.3451 |

*Table 21. PCC of changes of vegetation in the altitudinal zones due to relative humidity.*

| Change of vegetation due to air temperature through Pearson correlation coefficient | | | | | |
|---|---|---|---|---|---|
| **Altitudinal zone** | **Annual variation** | **Q1** | **Q2** | **Q3** | **Q4** |
| 1 | 0.4826 | 0.3039 | 0.5129 | 0.4760 | -0.0187 |
| 2 | 0.3655 | 0.5297 | 0.5521 | -0.1223 | -0.5645 |
| 3 | 0.0229 | 0.3040 | 0.1688 | -0.6973 | -0.4601 |
| 4 | -0.2575 | 0.2215 | -0.2415 | -0.7188 | -0.4738 |

*Table 22. PCC of changes of vegetation in the altitudinal zones due to air temperature.*

| Change of vegetation due to radiation through Pearson correlation coefficient | | | | | |
|---|---|---|---|---|---|
| **Altitudinal zone** | **Annual variation** | **Q1** | **Q2** | **Q3** | **Q4** |
| 1 | 0.2176 | 0.5500 | 0.1754 | -0.1139 | 0.0827 |
| 2 | 0.1815 | 0.8614 | 0.4377 | -0.3215 | -0.3018 |
| 3 | -0.0029 | 0.2654 | 0.4256 | -0.2085 | -0.4726 |
| 4 | -0.0533 | 0.0375 | 0.1154 | 0.0452 | -0.2684 |

*Table 23. PCC of changes of vegetation in the altitudinal zones due to precipitation.*

## Principal Component Analysis (PCA):

The PCA was performed using the annual weather data and the changes in vegetation, the analysis was performed with a set of nine variables, the four annual averages of historical weather data, and five categories of change of vegetation throughout the period 2013-2020. The PCA operation reduced all the variance from the nine variables to seven principal components (PC).

Table 24 shows the values for Eigen vectors, each Eigen value represents the magnitude of the vector representing each component, cumulative percentage of variance is listed from most contribution to least. The Scree plot from figure 20 shows the percentage for data variance in each of the seven principal components.

| **Component** | **Eigenvalue** | **Percentage of variance** | **Cumulative percentage of variance** |
|---|---|---|---|
| 1 | 3.83 | 42.52 | 42.52 |
| 2 | 2.81 | 31.19 | 73.71 |
| 3 | 1.27 | 14.06 | 87.77 |
| 4 | 0.7 | 7.79 | 95.56 |
| 5 | 0.22 | 2.42 | 97.99 |
| 6 | 0.14 | 1.53 | 99.51 |
| 7 | 0.04 | 0.49 | 100 |

*Table 24. Eigen vectors values, percentage variance for each component, and cumulative percentage variance.*

Among all the generated components by the PCA, 87.77% of all the variance in the data is found within the first three components as shown in the above table, these three components represent the steepest growth in cumulative variance between the seven components, as it is shown in figure 20.

Principal component 1 accounts for 42.52% of all data variance, the variables that contribute more to this component are changes of vegetation in the second zone (20%), annual average relative humidity (16%), annual average air temperature (15%), annual precipitation (15%), gross change of vegetation(13%) and changes of vegetation in the first zone(13%). PC 2 accounts for 31.2% of all data variance, the variables that had more contribution in this component are changes of vegetation in the third and fourth zone, with both contributing 32% and 33% respectively of the PC variance, gross change of vegetation, and changes of vegetation in the first zone had contributions of 15% and 13% respectively also for PC 2 variance. PC 3 variance is mostly due to annual average radiation with 50% of the PC variance, Annual average air temperature has also a significant contribution in the PC, with 19% of the PC variance.

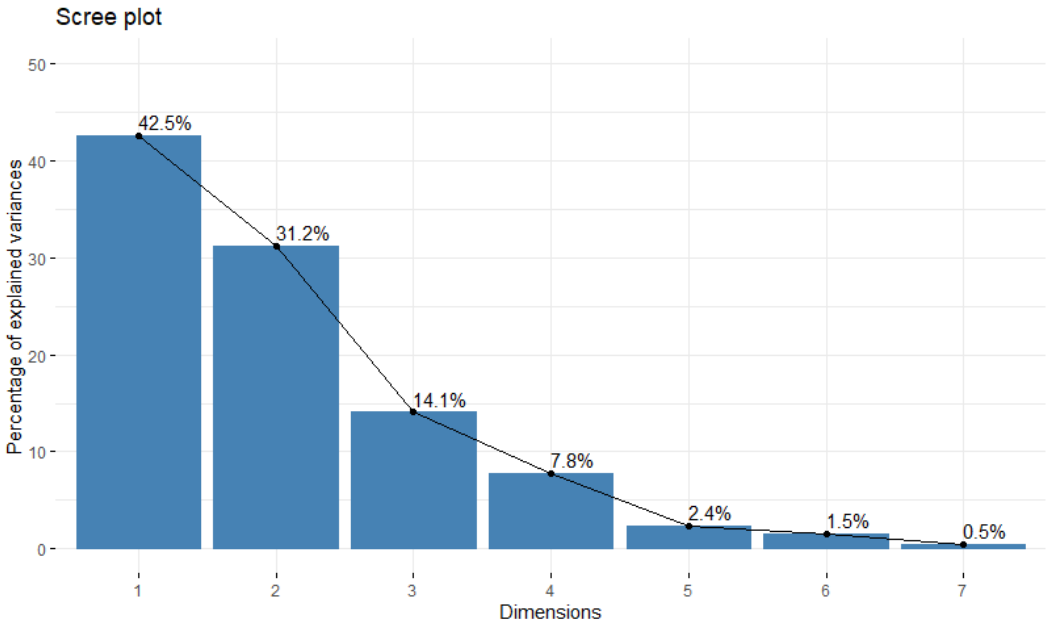


*Figure 20. Variance percentage for each of the seven principal components.*

### Variables contribution to components

Within the PCA, each principal component (PC) represents a linear combination between the different variables of the system, having each variable a different contribution in the PC. Percentage contribution for each variable across the first 5 PC is shown in table 25.

| Variable | Component 1 | Component 2 | Component 3 | Component 4 | Component 5 |
|---|---|---|---|---|---|
| Annual average air temperature | 14.98 | 0.97 | 18.90 | 10.93 | 23.55 |
| Annual average relative humidity | 16.25 | 1.96 | 7.48 | 24.48 | 2.25 |
| Annual precipitation | 14.58 | 1.36 | 2.54 | 45.86 | 19.33 |
| Annual average radiation | 7.12 | 0.15 | 50.44 | 0.21 | 32.74 |
| Gross change of vegetation | 13.07 | 15.13 | 4.57 | 0.53 | 3.62 |
| Change of vegetation in zone 1 | 12.85 | 13.26 | 5.42 | 0.42 | 12.36 |
| Change of vegetation in zone 2 | 19.68 | 2.52 | 9.27 | 6.17 | 3.85 |
| Change of vegetation in zone 3 | 0.44 | 32.05 | 0.01 | 11.27 | 0.66 |
| Change of vegetation in zone 4 | 1.03 | 32.59 | 1.37 | 0.12 | 1.64 |

*Table 25. Principal components percentage contributions to the first 5 PC.*

## PCA for variables:

The variables contribution and correlation for PC 1 & 2 are shown in figure 21, the extent of the arrow indicates the magnitude of the vector representing the variable, the longer the arrow the more the variable contributed to the principal components. Positively correlated variables are grouped, while negatively correlated variables are opposite one to another.

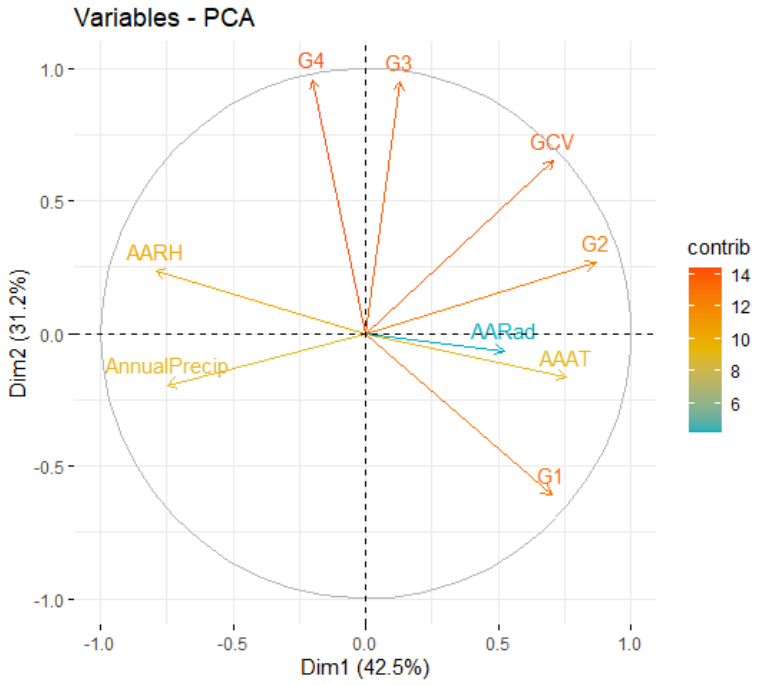


*Figure 21. Correlation circle of variables.*

Figures 22 and 23 show the contributions of the variables for the two principal components respectively. The threshold line for each bar represents a contribution above 11 % from the variable to the component.

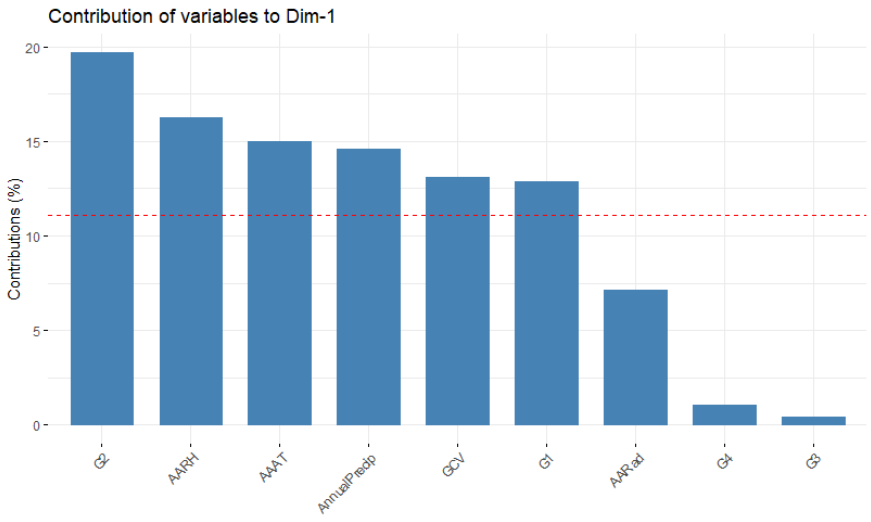


*Figure 22. Variables contributions to PC 1.*

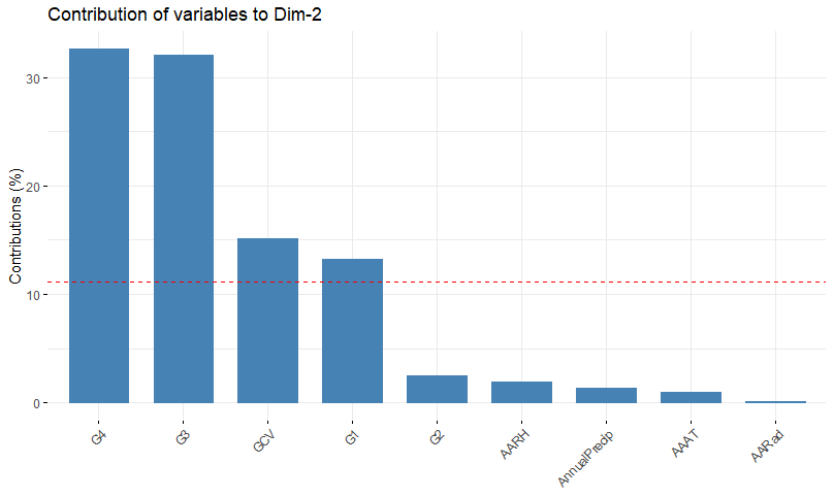


*Figure 23. Variables contribution to PC 2.*

## PCA for annual data:

Each year's contribution to the first 5 PC is shown in table 26. Also yearly data is shown below in figure 24 with its relative importance along with the first two principal components, where the horizontal axis corresponds to the first principal component, while the vertical axis represents the second principal component. Each individual in the graph represents a year of the studied period, being that point 1 represents 2013 until point 8 representing 2020. Cos 2 represents the square cosine for the squared coordinates of the data, it represents in the graph the quality of representation of the variables throughout the yearly data, a higher value indicates a better representation of the yearly data in the principal components.

| Year | Component 1 | Component 2 | Component 3 | Component 4 | Component 5 |
|---|---|---|---|---|---|
| 2013 | 1.80 | 1.83 | 0.03 | 49.71 | 19.48 |
| 2014 | 5.04 | 5.87 | 6.14 | 30.24 | 0.43 |
| 2015 | 37.02 | 9.14 | 0.01 | 0.36 | 0.11 |
| 2016 | 3.01 | 2.64 | 42.88 | 5.38 | 32.63 |
| 2017 | 18.71 | 28.71 | 0.41 | 0.15 | 11.90 |
| 2018 | 4.86 | 43.99 | 0.85 | 10.63 | 3.39 |
| 2019 | 29.41 | 6.16 | 2.62 | 2.81 | 1.48 |
| 2020 | 0.15 | 1.66 | 47.06 | 0.72 | 30.57 |

*Table 26. Yearly percentage contribution to the first 5 PC.*

Figure 24 represents the annual data variation across components 1 and 2 in the horizontal and vertical axis respectively. Each point represents the data variation for a year, point 1 represents 2013, and so on until point 8 accounting 2020. Years found closer to the origin have less representativity in the data variation (lower Cos 2 values), while points in the graph farther from the origin represent years that had more representation for the data variation. Two clusters are observed given this representativity trend for the annual data, first one corresponds to years with low representativity in data variation (1, 2, 4, and 8) which correspond to 2013, 2014, 2016, and 2020 respectively. The second cluster corresponds to years that had a bigger representation in the data (3,5, 6, and 7), these high representative years are 2015, 2017, 2018, and 2019.

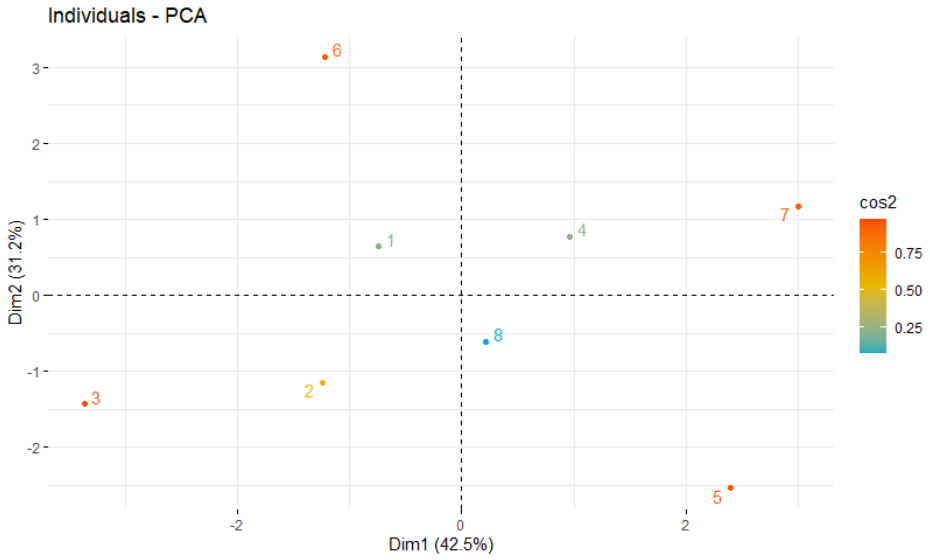


*Figure 24. Yearly representation of PC 1 & 2.*

Figure 25 shows the percentage contribution to PC 1 & 2, same cluster arrangement as figure 24 is observed, where of the 8 studied years, much representation of the data variation is found in four of them all shown above the threshold line (2015, 2017, 2018, and 2019).

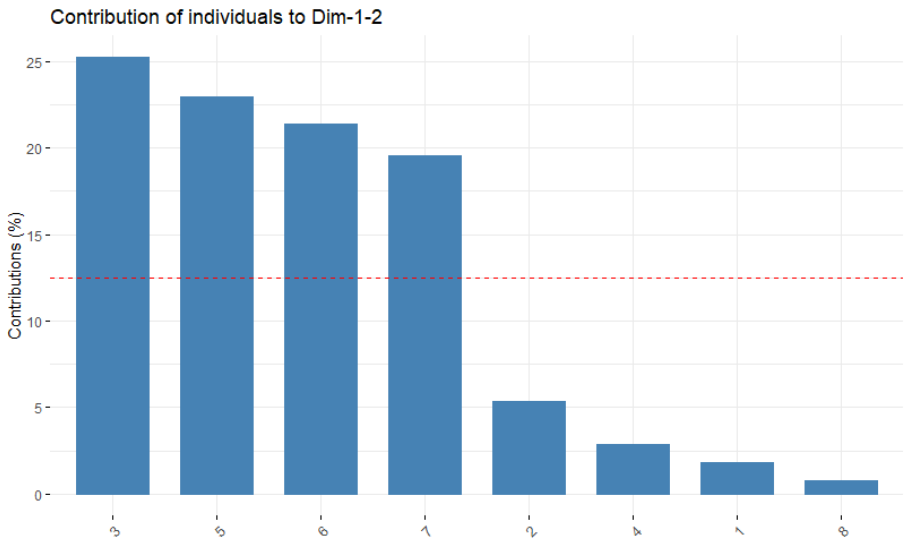


*Figure 25. Yearly percentage contribution to PC 1 & 2.*

# Discussion

## Chapter 1 analysis:

Soil components varied across the different forest structures and altitudes, the following discussion focuses on the concentrations of components when transitioning from one forest structure to another in locations that had bark beetle outbreaks but also in sites that have not seen these beetle migrations and how are these forests transitions happening at different altitudes. Results are compared to literature research relevant to components fluxes due to bark beetle outbreaks.

## Organic matter:

As Yavitt and Fahey, (1986) state, the transition of a green forest structure towards a yellow and grey structure results in the addition of material to the soil, the first horizon of the soil receives this input from first hand, increasing the amount of carbon within the soil. Overall, yellow and red structures had the highest amount of organic matter in the soil, the highest concentration of organic matter was detected in the first two zones (3300-3600masl) and decreases gradually when altitude increases. This trend is observed within all the analyzed structures, where organic matter content in soil decreases at higher altitudes.

The rate at which organic matter is released into soil components appears to vary, for zone 3 (3600-3800masl) the highest content was for grey forest structures, but the opposite trend was observed for the highest zone, where the green structure showed the highest content of organic matter. This difference in rates may be due to processes such as rhizodeposition and mycorrhizal interactions in yellow, red, and grey structures that decrease overall (Mikkelson et al. 2013; Xiong et al. 2011), so these variations in inputs and outputs of organic matter change the rate of organic matter accumulation as seen in figure 6.

## Total nitrogen:

Processes such as nitrification, denitrification, and mineralization are prone to change at the location where outbreaks existed (Mikkelson et al. 2013). Figure 8 shows a variety of trends, on the first hand, an overall increase in total nitrogen exists when transitioning from both green to a yellow structure and yellow to a grey structure. When analyzing by altitudinal zone, the first two zones are the ones that have a higher concentration of nitrogen in the soil, the highest nitrogen composition for these zones is for green forest structures.

Also, just as with organic matter, nitrogen composition in soil decreased when altitude increased through each zone. For the first three zones (3300-3800masl) the green structures soil organic horizon had higher nitrogen composition, while in the fourth zone the highest concentration existed in the grey structure. This inconsistency of a general trend may be explained by Huber et al. (2004) by the fact that nitrogen sinks in soil may not be enough to compensate nitrate losses by the lack of root uptake and by the fact that the decay of litter and wood from outbreak sites may take considerable time depending on the sites conditions.

## Total phosphorus:

Phosphorus change in components increased in overall concentrations when transitioning through forest structures. This increase was also consistent for each of the zones, as the phosphorus concentration in grey structures was highest of all structures and green structures had the lowest concentrations for all zones. Opposed to organic matter and nitrogen, the highest phosphorus concentrations were for the upper zones. This could be due to a higher ash input in higher zones from Colima Volcano, which is active, though the highest concentration was in zone 3 and not the uppermost. When comparing total phosphorus of green structures with grey structures concentrations quadrupled for the first two zones and almost doubled for zones 3 and 4.

## Soil cation exchange capacity:

It was observed for all the four studied cations that the overall average concentrations increased when transitioning from a green forest structure towards a yellow structure.

This middle structure transition appeared to have greater cation exchange capacity. The increase in CEC can partly be due to the material added in the first soil horizon when tree material falls from dead trees (Yavitt and Fahey. 1986). This result may also be coupled to other processes relevant to other components, such as nitrification which may end up in the formation of negatively charged nitrate that may attract these positively charged ions (Huber et al. 2004, Tokuchi et al. 2004). pH changes can also have a direct impact on the cations present in the soil of different sites, which may result in loss of base cations (Mikkelson et al. 2013) as it is seen in much of the analyzed grey structures, where the cation concentration decreases with respect the yellow and red structures.

Regarding the potassium response for forest transitions, Kana et al. (2012) found a rapid response of this component as a result of the decaying material released by dead trees, in this study, potassium increased for the yellow structures, which is the first transition of sites that had beetle outbreaks, this might correspond to the decaying material input as stated by Kana et al. (2012).

Calcium response in forest transitions also appears to be consistent with Kana et al. (2012) study, as the slower increase through forest transitions resulted in a slight increase of calcium in grey sites in comparison to the yellow and red locations.

### Soil humidity content:

Overall, humidity increased in locations where beetle outbreaks existed, for all of the forest structures and altitude zones, the highest humidity content was found in yellow and red structures and the lowest humidity content was found in green structures, displaying similar concentrations behavior overall and between each zone. Soil moisture increase has been reported by Mikkelson et al. (2013) study and is consistent with the observations from the VCC soil samples.

Woods et al. (2006) reported that increases in soil humidity can be coupled to processes regarding the death of the trees, as transpiration from trees decreases after the dying of the pines, this seems consistent with the increase in humidity content for samples corresponding to yellow and red structures.

### pH:

Changes in pH are coupled to a variety of processes regarding the change of the components in the organic soil horizon. A decrease in soil pH might occur after sectors of pine die during the transition of forest structure (Hélie et al. 2005). On the other hand, increases in soil pH have been studied for sites with the presence of bark beetle, Xiong et al. (2011) and Kana et al. (2012) studies reported increases in soil pH, a process which is coupled within the dissolved organic carbon of the soil.

Both cases were observed for this study, on the overall average, pH decreased because nitrogen component was measured as total nitrogen, it cannot be attributed to an increase of nitrification, what can be said, is that for zones 1 and 2, pH increased, it was within these two zones that organic matter in the soil had greater concentration, so this increase in pH might be due to the increase in dissolved organic carbon, as stated by Xiong et al. (2011) and Kana et al. (2012).

## Chapter 2 Analysis:

Most of the changes within forest structures in the high mountain (above 3300 masl) can be attributed to the bark beetle-pine dynamic. These changes at these altitudes correspond mostly to forest sectors dominated by *Pinus Hartwegii*. Abies conifer species are found in certain sectors at the low parts of the high mountain (in lower abundance than the pine and near drainage areas). Though spectral signatures and the vegetation indexes don't distinguish pines from Abies, both conifers, forest transitions, and changes of vegetation are attributed to these dynamics. This is because Abies population has not seen a natural predator at the VCC such as the pine and the bark beetle and that it is rarely found above 3500 masl.

Therefore, changes perceived in the false-color composite images were attributed to the dying of the pines caused by the bark beetle. Given this, the vulnerability analysis focuses on the forest structure transitions of *Pinus Hartwegii* forest sectors as a result of bark beetle migrations over different locations in the high mountain. Though this consideration is the main approach for the recent transitions in forest structures (2012-2020) as there are currently no significant anthropogenic alterations, it will not be the same for the interpretation of forest transitions in the 90's decade.

According to mountain management, intensive agriculture along with constant wood extraction existed in the high mountain during the decade of the 90s as well as previous decades. Sanitation practices as they were called, extracted the wood with the excuse of stopping the beetle migrations. The result of these practices was a considerable amount of bare soil and sectors with only alpine meadows. Figure 15 shows an initial high mountain status for our studied period with approximately equal areas of green vegetation and yellow and grey vegetation. This vegetation status kept quite constant until the early 2000s, when an increase in green vegetation is highly noticeable by the remote sensors, going from 1885 hectares of green vegetation in 1999 to a record maximum of 2529 hectares in 2010. This transition of yellow and grey structures towards green structures correlates in time to the retrieval of cattle and agriculture livestock as well as ending up with the sanitation practices.

This trend in the whole region of study is consistent when analyzing by altitudinal zones (figure 16), all of the four zones appear to have a constant area of green and yellow and grey structures during the 90's decade and start increasing towards a green forest structure after 2000. This transition increase was most significant for the second, third, and fourth zone (3400-4270 masl), the second zone had a transition from 654 hectares of green vegetation in 2001 to a record of 1079 hectares in 2015. Respectively, the third zone had a transition of 244 hectares in 1999 to 521 hectares by 2015, which represents an increase in the area of more than 100% concerning its lowest. Lastly, the fourth zone had also a considerable increase in green forest structure for that period, having an increase of 69 hectares in 1999, to twice that area (138 hectares) by 2017. These altitudinal zones represent the area covered with the highest density of *Pinus Hartwegii.*

After 2014, bark beetle outbreaks increased in magnitude, resulting in a continuous increase towards yellow and grey forest structures marked by a continuous decrease of green vegetation structure perceived in the remote sensing. This change perceived by the false color vegetation indexes is attributed largely to bark beetle migrations and outbreaks. Again, the zones that had a more significant change are the second, third, and fourth zones.

Though variations in the alpine terrain are minor, these can be attributed to change in tree coverage. Bare soil with a high content of sand was classified as alpine terrain, as the reflectance of the bare soil and the sandbanks of the volcano and higher parts of the mountain are very similar and as a result, spectral signatures are close one to another.

The following analysis corresponds to the statistical tests correlating these late forest transitions (2013-2020) to weather and climate parameters. It appears that for the last 8 years there is a stronger correlation between the changes of vegetation and the weather and climate conditions in the high mountain pine-beetle dynamic in the first 6 months of the year and mostly in the altitudinal zones comprehended between 3300 masl and 3600 masl, this interpretation is a result of the PCC and PCA conducted and is furtherly discussed.

### PCC analysis:

The PCC analysis with the weather data and changes of vegetation data showed that decreases in relative humidity and precipitation and increases in air temperature and radiation are correlated to changes of vegetation in the first two altitudinal zones. Most of the higher correlations between variables exist between these two zones (1 & 2) where 11 of 17 PCC with an absolute value above 0.5 corresponded to these zones(all correlations above absolute 0.5 are shown in the table below). In the third quartile, two correlations showed the contrary dynamics, as a decrease in air temperature correlated to changes in vegetation in the upper zones of the mountain (3600-4260 masl).

This statistical analysis and the correlations showed are consistent with studies by Kurz et al. (2008) and Williams and Liebhold (2002), they showed that changes in climate such as warmer periods in winter and summer, as well as a reduction in rainfall, are drivers for this outbreaks, altering the natural state of this dynamic.

Relationships between variables with a value above absolute 0.5000 are shown in the table below as they are considered to show a correlation between the variables. Positive values denote a direct relation while negative values represent an inverse relation.

| Pearson correlation value | Independent variable | Dependent variable |
|---|---|---|
| -0.7097 | Annual average relative humidity | Change of vegetation within 3300-3400 masl.<br><br>A decrease in annual average relative humidity is correlated to a change of vegetation in the 3300-3400 masl altitudinal zone. |
| -0.6317 | Annual average relative humidity | Change of vegetation within 3400-3600 masl.<br><br>A decrease in annual average relative humidity is correlated to a change of vegetation in the 3400-3600 masl altitudinal zone. |
| -0.7361 | Annual precipitation | Change of vegetation within 3400-3600 masl.<br><br>A decrease in annual precipitation is correlated to a change of vegetation in the 3400-3600 masl altitudinal zone. |
| 0.5841 | Q1 air temperature | Gross change of vegetation.<br><br>An increase in air temperature in the first quarter of the year is correlated to the gross change of vegetation. |
| 0.5297 | Q1 air temperature | Change of vegetation within 3400-3600 masl.<br><br>An increase in air temperature in the first quarter of the year is correlated to the change of vegetation in the 3400-3600 masl altitudinal zone. |
| 0.5521 | Q2 air temperature | Change of vegetation within 3400-3600 masl.<br><br>An increase in air temperature in the second quarter of the year is correlated to the change of vegetation in the 3400-3600 masl altitudinal zone. |
| -0.6973 | Q3 air temperature | Change of vegetation within 3600-3800 masl.<br><br>A decrease in air temperature in the third quarter of the year is correlated to the change of vegetation in the 3600-3800 masl altitudinal zone. |
| -0.7188 | Q3 air temperature | Change of vegetation within 3800-4260 masl.<br><br>A decrease in air temperature in the third quarter of the year is correlated to the change of vegetation in the 3800-4260 masl altitudinal zone. |
| -0.6871 | Q1 Relative humidity | Change of vegetation within 3400-3600 masl.<br><br>A decrease in relative humidity in the first quarter of the year is correlated to the change of vegetation in the 3400-3600 masl altitudinal zone. |
| -0.6137 | Q1 Relative humidity | Gross change of vegetation.<br><br>A decrease in relative humidity in the first quarter of the year is correlated to the gross change of vegetation. |
| -0.6334 | Q2 Relative humidity | Change of vegetation within 3300-3400 masl.<br><br>A decrease in relative humidity in the second quarter of the year is correlated to the change of vegetation in the 3300-3400 masl altitudinal zone. |
| -0.6083 | Q2 Relative humidity | Change of vegetation within 3400-3600 masl.<br><br>A decrease in relative humidity in the second quarter of the year is correlated to the change of vegetation in the 3400-3600 masl altitudinal zone. |

| | | |
|---|---|---|
| -0.5756 | Q2 Relative humidity | Gross change of vegetation.<br><br>A decrease in relative humidity in the second quarter of the year is correlated to the gross change of vegetation. |
| -0.5349 | Q2 precipitation | Gross change of vegetation.<br><br>A decrease in precipitation in the second quarter of the year is correlated to the gross change of vegetation. |
| 0.7720 | Q1 radiation | Gross change of vegetation.<br><br>An increase in radiation in the first quarter of the year is highly correlated to the gross change of vegetation. |
| 0.8614 | Q1 radiation | Change of vegetation within 3400-3600 masl.<br><br>An increase in radiation in the first quarter of the year is highly correlated to the change of vegetation in the 3400-3600 masl altitudinal zone. |
| 0.5548 | Q2 radiation | Gross change of vegetation.<br><br>An increase in radiation in the second quarter of the year is correlated to the gross change of vegetation. |

*Table 27. Pearson correlation coefficient between dependent and independent variables.*

**General trends of weather conditions and altitudinal changes of vegetation:**

Relative humidity: Annual average relative humidity correlates with changes of vegetation in the altitudinal zones of 3300-3400 masl and 3400-3600 masl, exerting a greater influence at the 3300-3400 masl zone. In the first two quartiles, a decrease in relative humidity correlated to changes in vegetation mostly in the area between 3300-3600masl.

Precipitation: Changes in vegetation correlated with decreased precipitation, the annual precipitation changes showed a strong correlation in the vegetation changes of the 3400-3600 masl zone. The second and third quartiles also showed strong correlations with a decrease of precipitation in the altitudinal zones between 3300-3600 masl.

Air temperature: An increase in temperature in the first two quartiles showed a correlation with changes of vegetation mostly in the altitudinal zone of 3400-3600 masl. The higher parts of the mountain showed the contrary, a decrease in temperature in the third quartile showed a correlation to changes of vegetation between the 3600-4260 masl.

Radiation: Only in the first two quartiles does radiation appears to exert an influence on the changes of vegetation, showing a strong correlation in the first quartile in the overall gross change of vegetation and the 3400-3600 masl zone.

Given this trends of how weather parameters appear to act as drivers for this dynamic in the different altitudinal zones, this study is consistent with the fact that indeed, climate change and weather parameters contribute to this dynamic (Carroll et al, 2004) of *Pinus Hartwegii* and *Dendroctonus adjuntus* at the VCC

## PCA variables analysis:

Figure 21 shows how variables are correlated between them for the data variation, annual precipitation, and relative humidity are negatively correlated to changes of vegetation in the first and second zone, denoting that a decrease in annual precipitation and a decrease in relative humidity are highly correlated to vegetation transitions from green vegetation to yellow vegetation in this zones.

The Gross change of vegetation and vegetation changes in the second zone is closely correlated as they show closeness in figure 21. The same is true for changes of vegetation in the upper mountain zones, where changes in the third and fourth zone are highly correlated with each other. Contrary to this, changes in these zones (3 & 4) show no correlation with changes in the zones below (1 & 2). Annual average air temperature shows a positive correlation with changes in the first zone as well as changes in the second zones. Annual precipitation had little representation in the changes of vegetation for the third and fourth zone

Annual average radiation has the least contribution in the data variance for PC 1 and 2, while annual average relative humidity, annual precipitation, and annual average air temperature had similar contributions. All changes of vegetation had similar contributions along with the two PC.

**PCA yearly analysis:**

Two main clusters can be identified within the yearly data in the PCA relevant to the contributions in PC 1 & 2 as it is shown in Figure 25. Each cluster represents 4 years of data, cluster 1 can be seen as the four variables that had a similar and significant contribution to these PC's, being these years three (2015), five (2017), six (2018), and seven (2019). Each one of these yearly data had a contribution of more than 15% to the variation of the components. On the other hand, cluster 2 is composed of years one (2013), two (2014), four, and eight (2020), where each of these contributed less than 7% to the variation of the components. Cluster 1 is seen in figure 2 as the four outer points in the graph, while cluster 2 represents the closest points to the origin in the graph. For figure 3, cluster 1 is shown as the individuals above the threshold line (12.5% of variation), and cluster 2 is the individuals beneath the threshold line.

Being that clusters represent data variance, it can be said that cluster 1 (2015, 2017, 2018, 2019) accounts for the years that have brought more changes of vegetation in the mountain in the studied period (2013-2020). 2015 appears in figure 21 with a negative relative value in both components, this was the year that saw the most area transitions from yellow or grey vegetation to green vegetation, with a total of 187 hectares recovered to green vegetation. 2019 on the other hand, contributed significantly to the data variance as well, in figure 21 the graph shows a positive relative value across both components, this was the year with the highest green to

yellow vegetations transitions where 123 hectares changed from status in the second altitudinal zone only, and 290 hectares in the total studied area.

## Conclusion:

The research aimed to understand the natural dynamic of the pine-beetle in the high elevation forest of VCC in Mexico. This research firstly hypothesized that soil components would change due to beetle-pine interactions at different altitudes. And secondly, pine-beetle interactions would be driven by climate and weather changes. Consequently, a full methodology was proposed to find relevant evidence of beetle-pine interactions and their effect on soil and weather interactions.

The methodology proposed consisted first of a geochemical components characterization for several locations and altitudes at VCC. In total 39 sites were selected and sampled according to beetle migration and pine dieback. Three structures were defined accordingly to the dieback times. 1) Green structures: untouched regions; 2) Yellow and red structures considered zones with past presence of bark beetle resulting in pines with yellow and red needles; 3) Grey structures: forest with heavy needle and branches loss.

The geochemical characterization suggested differences in soil components between forest structures. Yellow and red forest structures had the overall higher concentrations of organic matter, potassium, sodium, and humidity content. And grey forest structures had the overall higher concentrations of nitrogen, phosphorus, calcium, and magnesium. These results proved the hypothesis that components change through forest transitions mostly due to organic matter deposition due to the dieback of trees.

The second part of the research was aimed to test how much of this dynamic is driven by climate and weather changes. To do so, a correlation of weather parameters and vegetation changes was analyzed. Historical weather data was gathered and forest transitions were modeled as changing vegetation areas with the use of remote sensing. It was found that a decrease of rainfall and relative humidity along with an increase in temperature and radiation positively correlated to forest transitions changes from green structures towards yellow, red, and grey structures simultaneously across the different altitude zones.

The natural and complex dynamic between *Dendroctonus Adjuntus* and *Pinus Hartwegii* at the VCC has lately intensified in magnitude and altitudes, these late outbreaks have caused the dieback of big forest sectors responding partly as a climate-driven dynamics, confirming the statements of several authors concerning beetle dynamics and climate.

Several measures have been considered to understand and fight against beetle-pine interactions by different interested sectors at VCC. The traditional management approach follows a sanitation practice. This practice consists in death biomass removal within beetle-presence sites, which its effectiveness has been questioned by scholars (see Kaňa. et al 2012; Jonášová, et al. 2004; Jonášová et al. 2007). Further management recommendations from this research to local authorities would be to keep untouched beetle-presence sites for natural biomass deposition. This aligns with the recommendation of Jonášová, et al. (2004); Jonášová et al. (2007) to follow non-intervention strategies rather than any technical forestry intervention.

The next step of this research is to determine if grey areas after total biomass deposition will follow a natural regeneration or whether the correct approach will be a technical intervention such as reforestation, and when is the appropriate time to do it.

Climate change will continue to be a challenge for the national park in regards to this dynamic, which as the study reveals it might be driven by weather parameters. This ancient dynamics will continue to exist in the park and it will be more perceptible and obvious at high elevations. Research should push towards understanding the specific relations that govern the two species of interest through time to understand nature's role in self-regeneration.

### Things to furtherly discuss:

There is only one station measuring weather conditions in the high mountain, found at 3461 masl. Weather conditions taken from the station are assumed to be the same for the study area while correlating changes of vegetation with weather data.

Since much of the year there is high cloud cover over the national park there is no exact consistency between the studied seasons of the weather data with the data of changes of vegetation obtained by maps. Most of the imagery selected was from the period between December and February.

A k-means clustering operation was computed in R, it was not selected for interpretation as all clusters created had no sense for the data. Weather data is always clustered with weather data, while a change of vegetation is always clustered with changes of vegetation. There was no way to interpret a relationship between dependent and independent variables.

NDVI indexes were created when imagery was being processed, but changes of vegetation were more visible using the false-color composite image rather than the whole operation of the NDVI. Other indexes could be furtherly used to correlate consistency with the used false color index.

All variable data is found in the Appendix, dependent variables comprehend the period 1989-2020, though only the period of 2013-2020 was used for the correlation between variables. Independent variable data consists of meteorological historical data from the water office climate station (3461 masl) has been compiled from the period 2013-2020. The station takes measurements every 10 minutes, averages were created compiling data every two weeks, resulting in 24 fortnights in annual tables from 2013-2020, seasonal averages were created with the resulting yearly tables.

## References:


Bentz, B.J., Logan, J.A., Amman, G.D., 1991. Temperature-dependent development of mountain pine beetle and simulation of its phenology. Canadian Entomologist 123, 1083–1094

Bray RH, Kurtz LT (1945) Determination of total, organic, and available forms of phosphorus in soil. Soil Sci 59:39–45

Bremmer JM (1965) Total nitrogen. In: Black CA (ed) Methods of soil analysis. Part 2 Agronomy. American Society of Agronomy, Madison, pp 1149–1178

Carroll, A. L., Taylor, S. W., Régniere, J., Safranyik, L., & Shore, T. (2004). Mountain pine beetle symposium: challenges and solutions. *Victoria, BC: Natural Resources Canada*, 223-232.

Creeden, E.P, Jeffrey A. Hicke, J.A, Polly C. Buotte, P.C, 2013. Climate, weather, and recent mountain pine beetle outbreaks in the western United States. Forest Ecology and management 312, 239-251.

Cullings KW, New MH, Makhija S, Parker VT (2003) Effects of litter addition on ectomycorrhizal associates of a lodgepole pine (Pinus contorta) stand in Yellowstone National Park.

Franceschi, V. R., Krokene, P., Christiansen, E., & Krekling, T. (2005). Anatomical and chemical defenses of conifer bark against bark beetles and other pests. *New phytologist*, *167*(2), 353-376.

Griffin JM, Turner MG, Simard M (2011) Nitrogen cycling following mountain pine beetle disturbance in lodgepole pine forests of greater yellowstone. For Ecol Manage 261(6):1077–1089

Griffin JM, Turner MG (2012) Changes to the N cycle following bark beetle outbreaks in two contrasting conifer forest types. Oecologia 170(2):551–565

Griffin JM, Simard M, Turner MG (2013) Salvage harvest effects on advance tree regeneration, soil nitrogen, and fuels following mountain pine beetle outbreak in lodgepole pine. For Ecol Manage 291:228–239

Hélie, J. F., Peters, D. L., Tattrie, K. R., & Gibson, J. J. (2005). Review and synthesis of potential hydrologic impacts of mountain pine beetle and related harvesting activities in British Columbia: Mountain Pine Beetle Initiative Working Paper 2005-23. *Natural Resources Canada, Canadian Forest Service, Victoria BC*.

Huber C, Baumgarten M, Go¨ttlein A, Rotter V (2004) Nitrogen turnover and nitrate leaching after bark beetle attack in mountainous spruce stands of the Bavarian forest national park. Water Air Soil Pollut Focus

Jonášová, M., & Prach, K. (2004). Central-European mountain spruce (Picea abies (L.) Karst.) forests: regeneration of tree species after a bark beetle outbreak. Ecological Engineering, 23(1), 15-27.

Jonášová, M., & Matějková, I. (2007). Natural regeneration and vegetation changes in wet spruce forests after natural and artificial disturbances. Canadian Journal of Forest Research, 37(10), 1907-1914.

Kaňa, J., Tahovská, K., & Kopáček, J. (2013). Response of soil chemistry to forest dieback after bark beetle infestation. Biogeochemistry, 113(1), 369-383.Prescott CE, Maynard DG, Laiho R (2000) Humus in northern forests: friend or foe? For Ecol Manag

Kurz, W. A., Dymond, C. C., Stinson, G., Rampley, G. J., Neilson, E. T., Carroll, A. L., ... & Safranyik, L. (2008). Mountain pine beetle and forest carbon feedback to climate change. *Nature*, *452*(7190), 987-990.

Lauer, W., 1973. The altitudinal belts of the vegetation in the central Mexican highlands and their climatic conditions. Artic Alpine Res. 5, 99–113.

Lauer, W., 1978. Timberline studies in central Mexico. Artic Alpine Res. 10, 383–396

Logan, J.A., Bentz, B.J., 1999. Model analysis of mountain pine beetle (Coleoptera: Scolytidae) seasonality. Environmental Entomology 28, 924–934.

Logan, J.A., Powell, J.A., 2001. Ghost forests, global warming and the mountain pine beetle (Coleoptera: Scolytidae). American Entomologist 47, 160–173. L

Lugo J, Martin del Pozzo A.L, Vázquez L (1992) Estudio geomorfológico del complejo volcánico de Colima

Mason, B. J. (1992). *Preparation of soil sampling protocols: sampling techniques and strategies* (No. PB-92-220532/XAB). Nevada Univ., Las Vegas, NV (United States). Environmental Research Center.

Mikkelson, K. M., Bearup, L. A., Maxwell, R. M., Stednick, J. D., McCray, J. E., & Sharp, J. O. (2013). Bark beetle infestation impacts on nutrient cycling, water quality and interdependent hydrological effects. *Biogeochemistry*, *115*(1-3), 1-21.

Miranda R, Chávez A, Navarro S, Villavicencio R (2009) Parque Nacional Nevado de Colima ; Contexto natural y paisajes

Mylavarapu, R., Sikora, F. J., & Moore, K. P. (2014). Walkley-Black Method. Soil test methods from the Southeastern United States, 158.

Rosén, K., Aronson, J. A., & Eriksson, H. M. (1996). Effects of clear-cutting on streamwater quality in forest catchments in central Sweden. Forest ecology and management, 83(3), 237-244.

Schulte EE, Hopkins BG (1996) Estimation of soil organic matter by weight loss-on-ignition. In: Magdoff FR, Tabatini MA, Hanlon EA (eds) Soil organic matter: analysis and interpretation. Soil Science Society of America, Madison

Solheim H. 1988. Pathogenicity of some Ips typographus-associated blue-stain fungi to Norway spruce. Meddelelser fra Norsk Institut for Skogforskning 40: 1–11.

Thomas GW (1982) Exchangeable cations. In: Page AL (ed) Methods of soil analysis. Part 2. Agronomy Monograph ASA and SSSA, Madison

Tokuchi, N., Ohte, N., Hobara, S., Kim, S. J., & Masanori, K. (2004). Changes in biogeochemical cycling following forest defoliation by pine wilt disease in Kiryu experimental catchment in Japan. Hydrological Processes, 18(14), 2727-2736.

Vité JP. 1961. The influence of water supply on oleoresin exudation pressure and resistance to bark beetle attack in Pinus ponderosa. Contributions from the Boyce Thompson Institute 21: 37–66.

Viveros-Viveros, H., Saenz-Romero, C., Vargas-Hernández, J. J., López-Upton, J., Ramírez-Valverde, G., & Santacruz-Varela, A. (2009). Altitudinal genetic variation in Pinus hartwegii Lindl. I: Height growth, shoot phenology, and frost damage in seedlings. *Forest Ecology and Management*, *257*(3), 836-842.

Williams, D. W., & Liebhold, A. M. (2002). Climate change and the outbreak ranges of two North American bark beetles. *The Bark Beetles, Fuels, and Fire Bibliography*, 34.

Wang X, Wang J, Zhang J (2012) Comparisons of Three Methods for Organic and Inorganic Carbon in Calcareous Soils of Northwestern China

Woods SW, Ahl R, Sappington J, McCaughey W (2006) Snow accumulation in thinned lodgepole pine stands, Montana. USA. Forest Ecology and Management 235(1–3):202–211

Xiong, Y., D'Atri, J. J., Fu, S., Xia, H., & Seastedt, T. R. (2011). Rapid soil organic matter loss from forest dieback in a subalpine coniferous ecosystem. *Soil Biology and Biochemistry*, *43*(12), 2450-2456.

## Appendix 1: Georeferenced sites for spectral signatures

| Reference point | Forest structure | Coordinates (decimal) | | Altitude (masl) |
|---|---|---|---|---|
| | | Latitude | Longitude | |
| 1 | 2 & 3 | 19.579485 | -103.600729 | 3514 |
| 2 | 2 | 19.578997 | -103.601293 | 3531 |
| 3 | 1 | 19.580677 | -103.597232 | 3440 |
| 4 | 1 | 19.576243 | -103.596387 | 3435 |
| 5 | 1 | 19.579315 | -103.609564 | 3722 |
| 6 | 1 | 19.580194 | -103.609166 | 3715 |
| 7 | 0 | 19.567431 | -103.617741 | 3944 |
| 8 | 2 | 19.570378 | -103.617092 | 3911 |
| 9 | 4 | 19.573925 | -103.620096 | 3861 |
| 10 | 4 | 19.571668 | -103.618012 | 3895 |
| 11 | 1 | 19.580391 | -103.616429 | 3776 |
| 12 | 2 | 19.577605 | -103.617957 | 3835 |
| 13 | 3 | 19.577611 | -103.617937 | 3836 |
| 14 | 0 | 19.577511 | -103.618431 | 3820 |
| 15 | 3 | 19.571684 | -103.605119 | 3500 |
| 16 | 4 | 19.577874 | -103.602305 | 3567 |
| 17 | 4 | 19.576357 | -103.603729 | 3588 |
| 18 | 4 | 19.574354 | -103.603750 | 3657 |
| 19 | 4 | 19.573019 | -103.604494 | 3718 |
| 20 | 4 | 19.580673 | -103.597151 | 3439 |
| 21 | 4 | 19.581694 | -103.602892 | 3466 |
| 22 | 4 | 19.580951 | -103.602819 | 3465 |
| 23 | 4 | 19.580784 | -103.601108 | 3466 |
| 24 | 0 | 19.568400 | -103.605379 | 3934 |
| 25 | 4 | 19.568383 | -103.612537 | 3807 |
| 26 | 3 | 19.568016 | -103.612422 | 3822 |
| 27 | 2 & 3 | 19.588561 | -103.597010 | 3391 |
| 28 | 2 & 4 | 19.589766 | -103.597809 | 3411 |
| 29 | 1 & 2 | 19.590312 | -103.598665 | 3420 |
| 30 | 2 | 19.589170 | -103.599142 | 3430 |
| 31 | 1 | 19.588302 | -103.599742 | 3442 |
| 32 | 2 | 19.588793 | -103.599220 | 3431 |
| 33 | 3 | 19.581535 | -103.632851 | 3525 |

| | | | | |
|---|---|---|---|---|
| 34 | 3 | 19.580792 | -103.631187 | 3542 |
| 35 | 4 | 19.580694 | -103.630042 | 3591 |
| 36 | 0 | 19.580325 | -103.630013 | 3600 |
| 37 | 2 & 3 | 19.574723 | -103.630801 | 3592 |
| 38 | 2 | 19.573928 | -103.630399 | 3597 |
| 39 | 4 | 19.572997 | -103.627657 | 3637 |
| 40 | 4 | 19.575666 | -103.626640 | 3666 |
| 41 | 0 | 19.576630 | -103.625891 | 3674 |
| 42 | 3 & 4 | 19.578997 | -103.623984 | 3698 |
| 43 | 4 bit of 3 | 19.580448 | -103.622897 | 3711 |
| 44 | 0 | 19.581425 | -103.621332 | 3725 |
| 45 | 0 | 19.582515 | -103.618812 | 3746 |
| 46 | 2 & 4 | 19.577363 | -103.618693 | 3818 |

*Table 28. Georeferenced sites for spectral signatures*

# Appendix 2

## Maximum likelihood classifications and False vegetation index maps

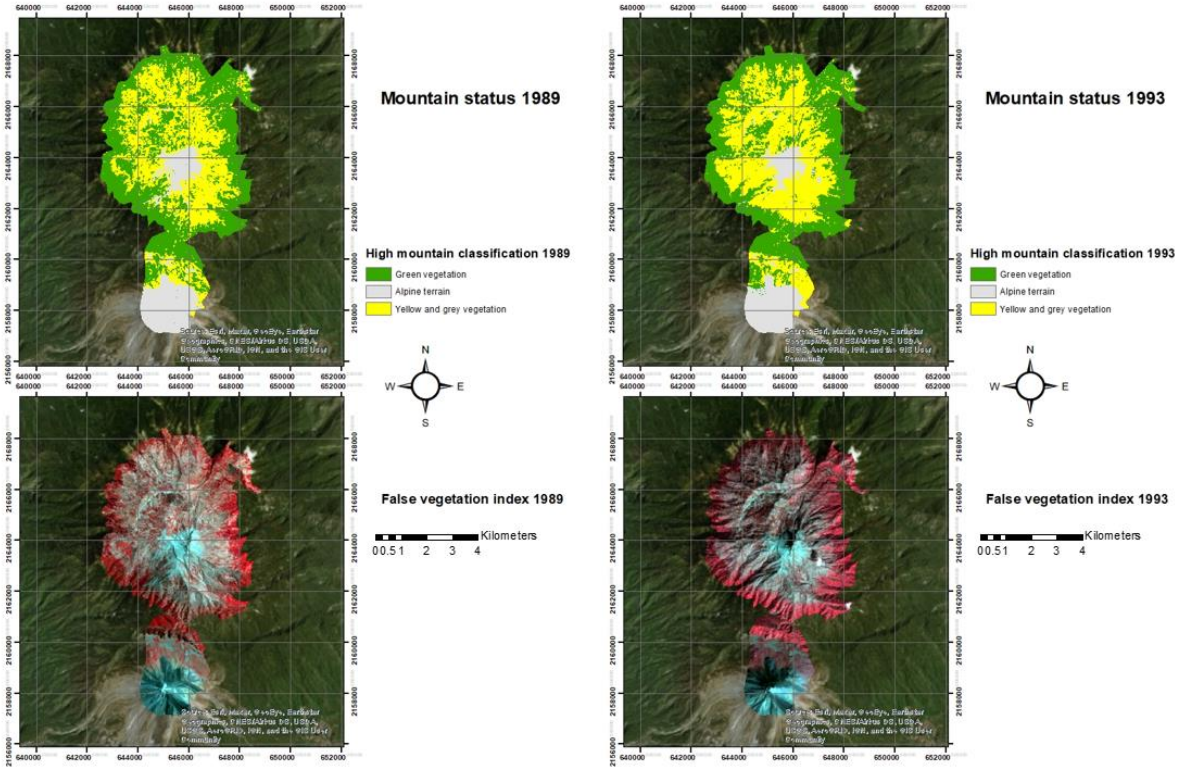


*Figure 26. 1989 and 1993 high mountain classification and false color vegetation index.*

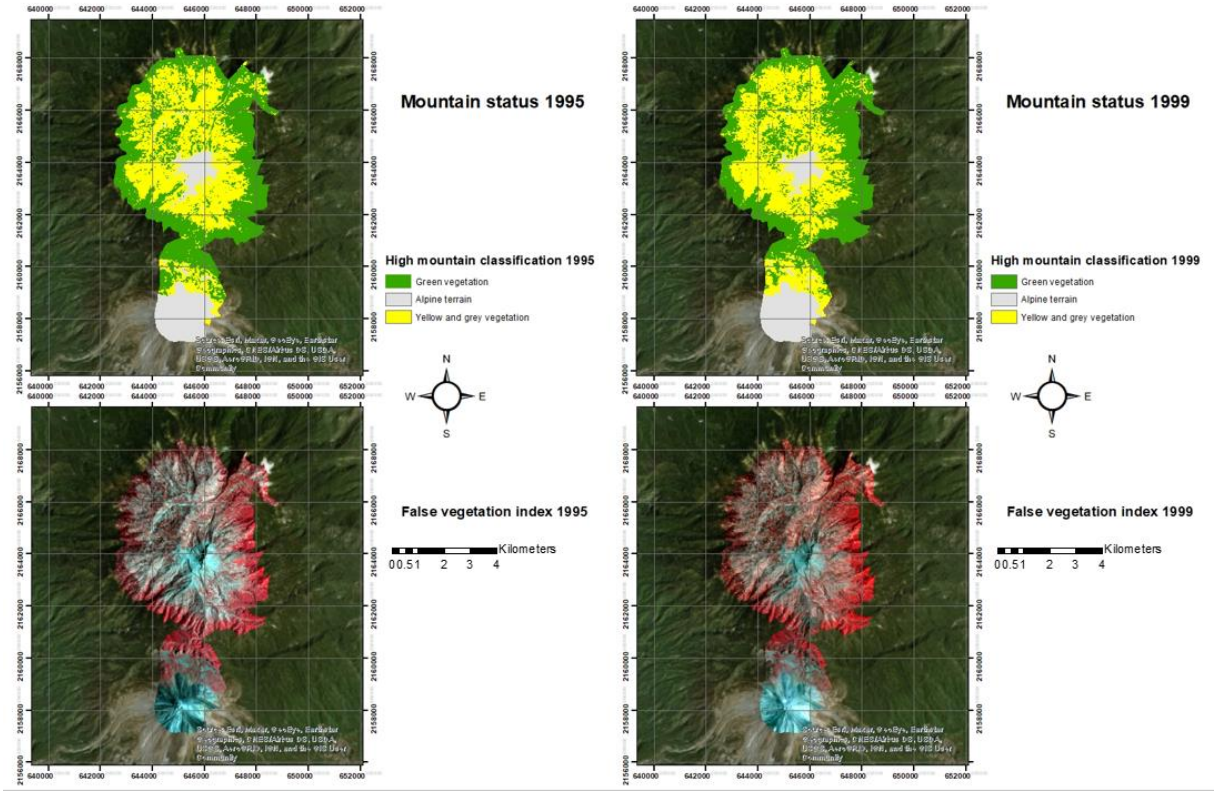


*Figure 27. 1995 and 1999 high mountain classification and false color vegetation index.*

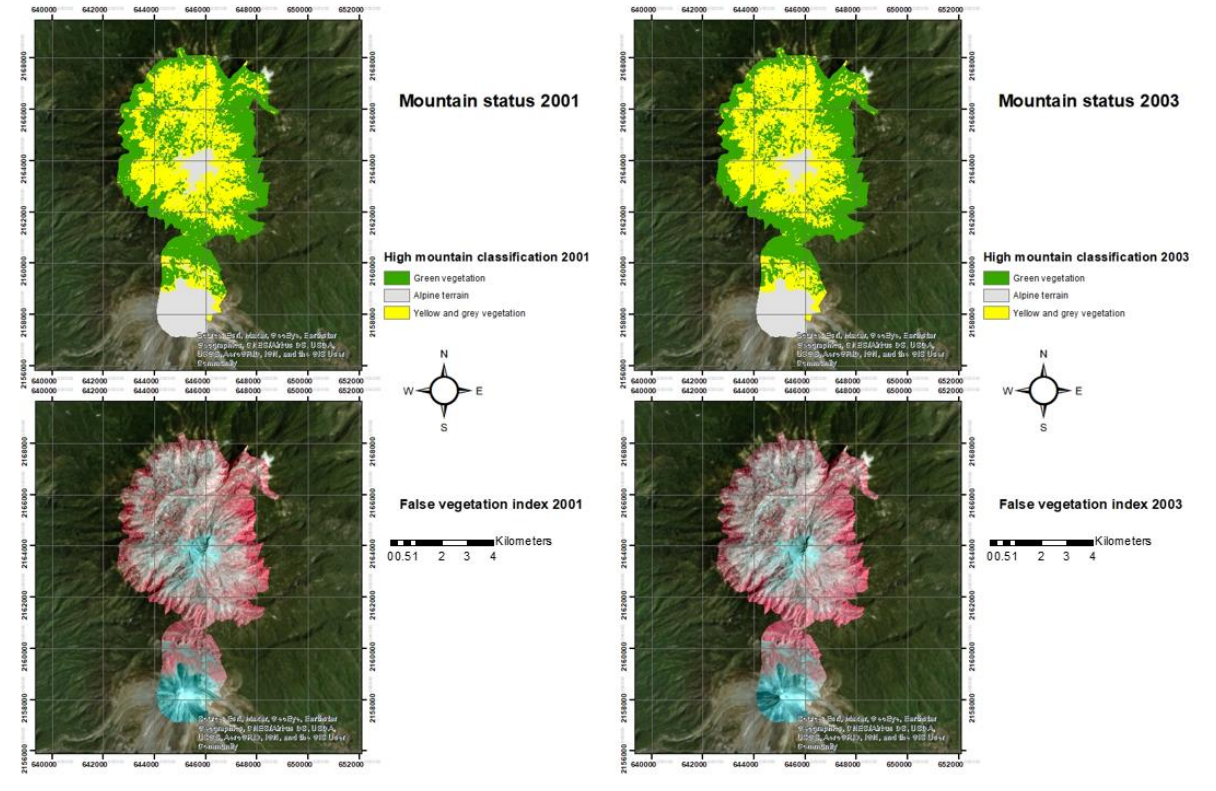


*Figure 28. 2001 and 2003 high mountain classification and false color vegetation index.*

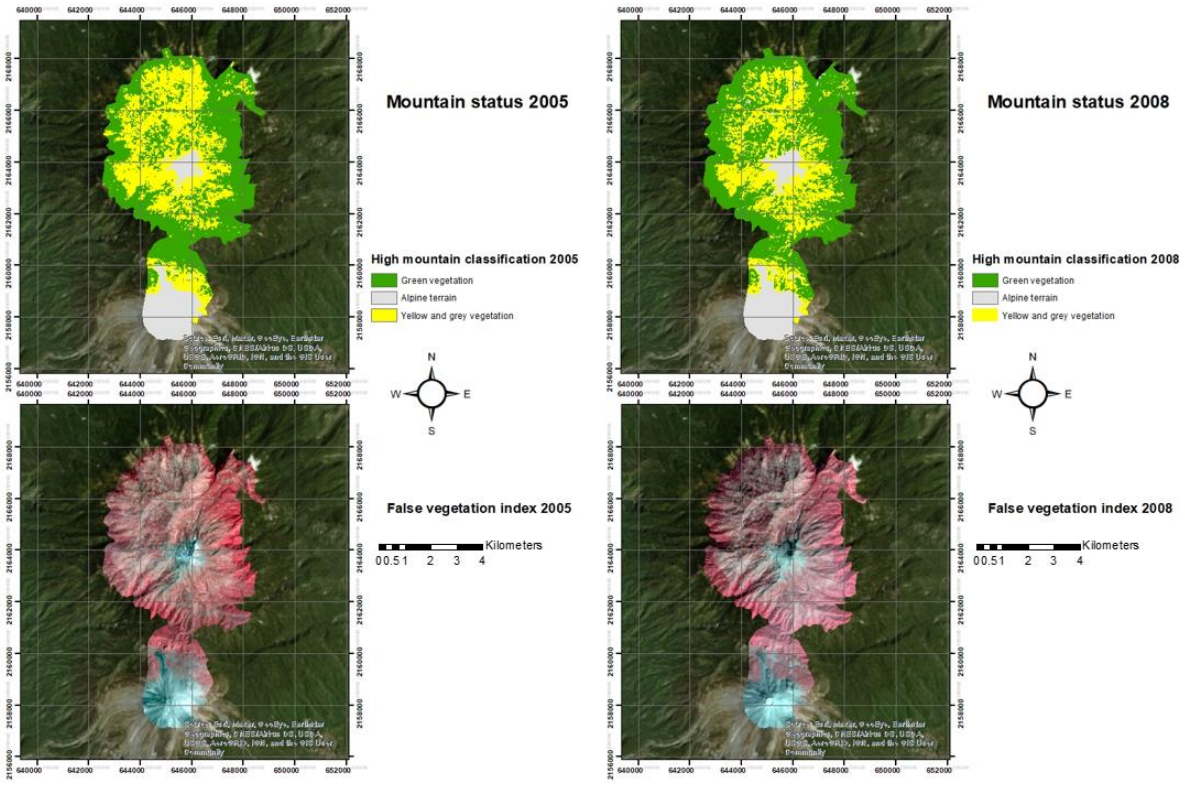


*Figure 29. 2005 and 2008 high mountain classification and false color vegetation index.*

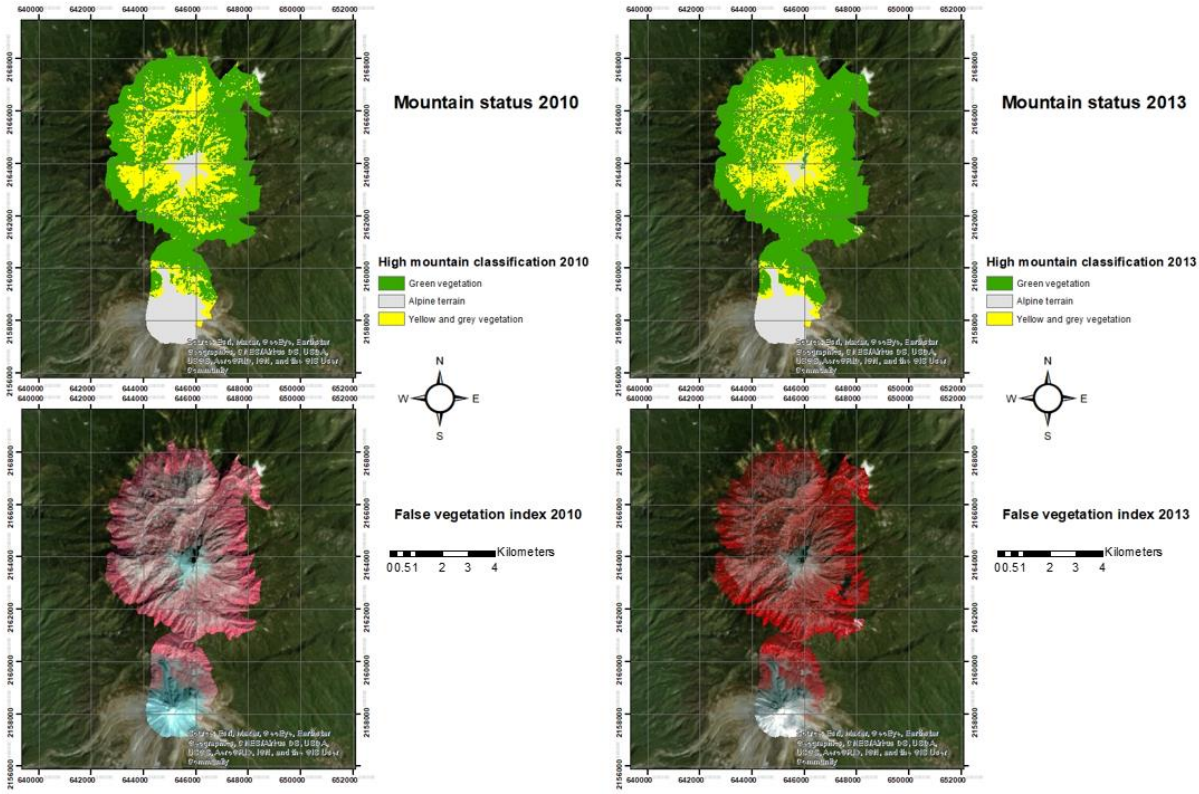


*Figure 30. 2010 and 2013 high mountain classification and false color vegetation index.*

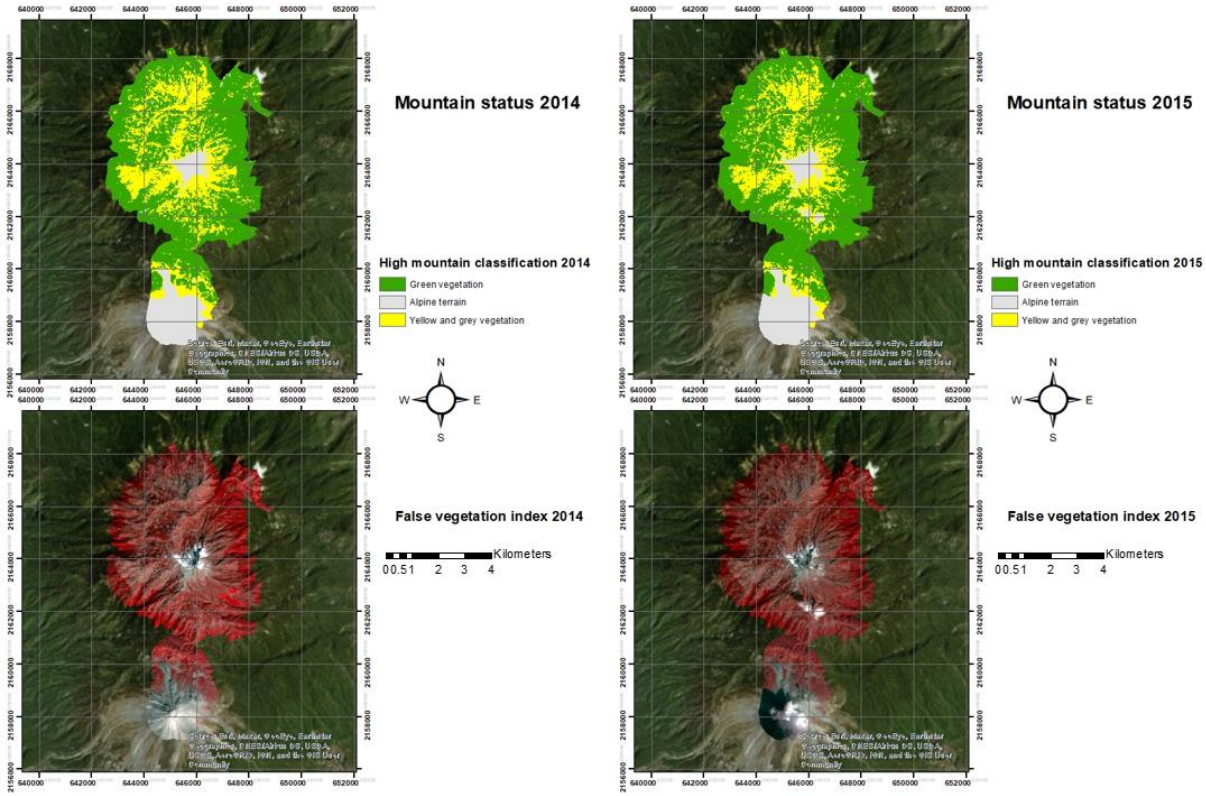


*Figure 31. 2014 and 2015 high mountain classification and false color vegetation index.*

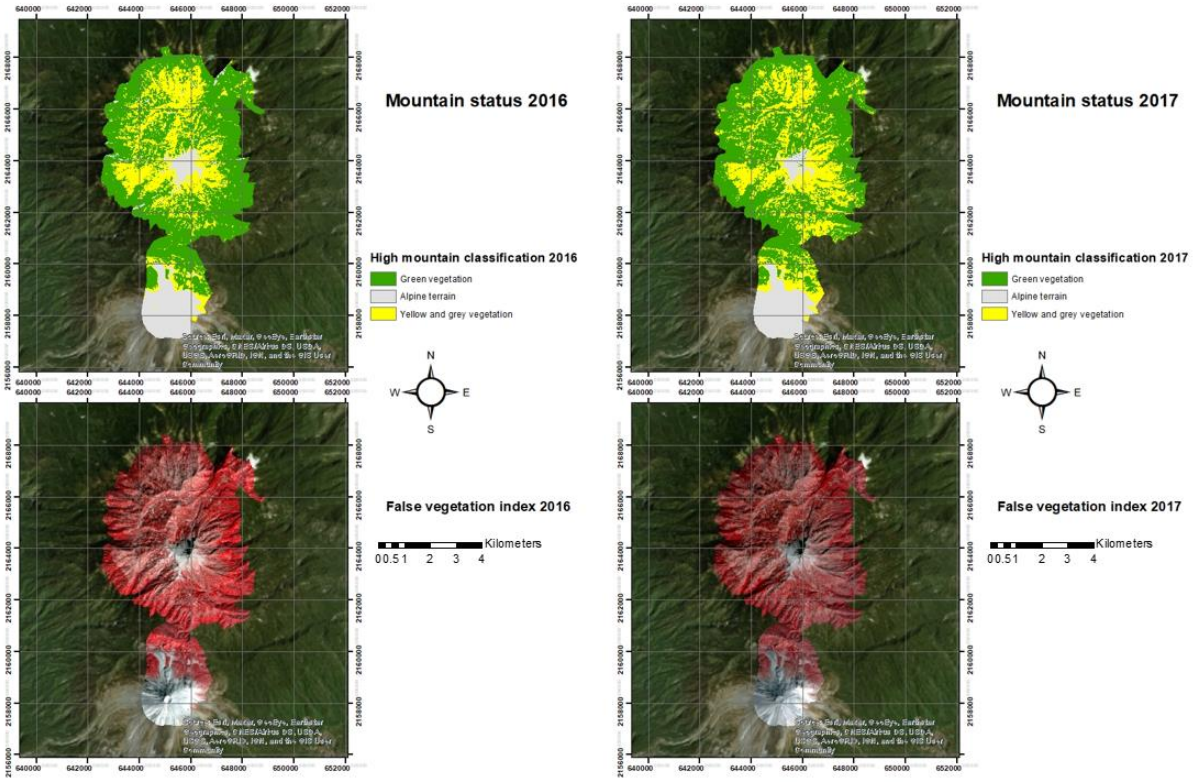


*Figure 32. 2016 and 2017 high mountain classification and false color vegetation index.*

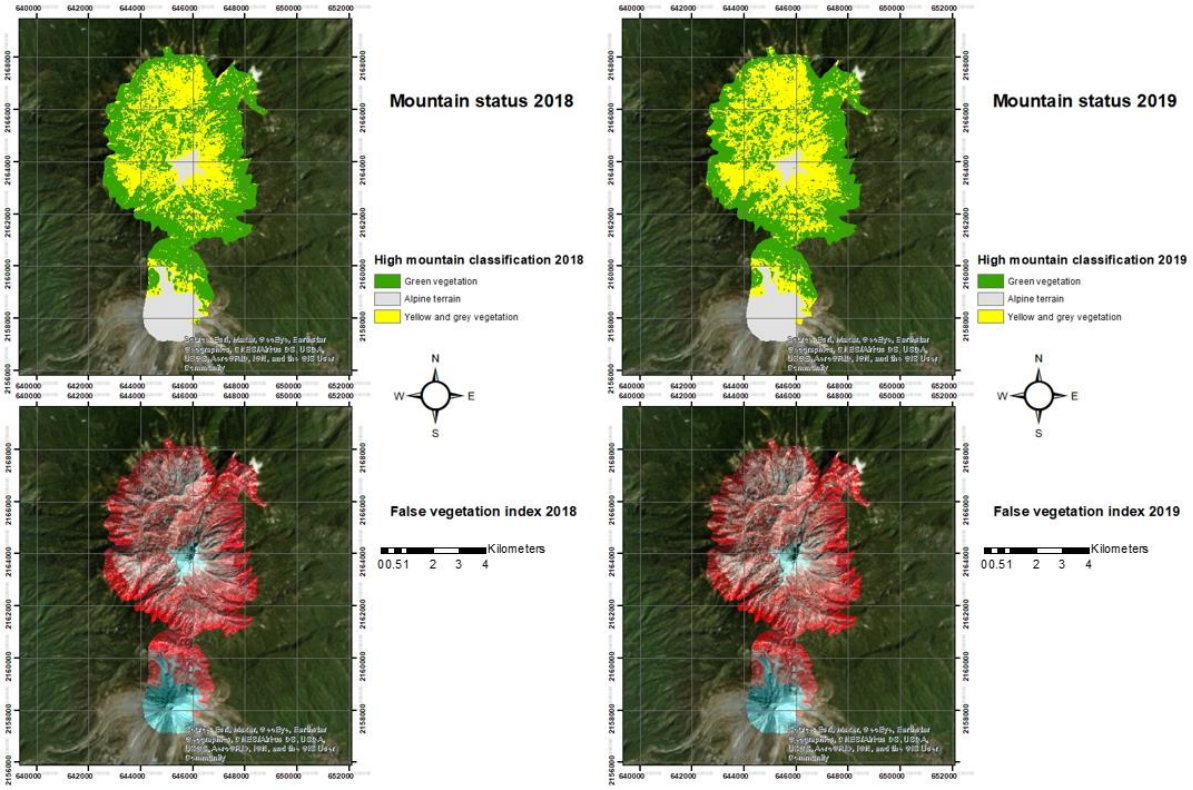


*Figure 33. 2018 and 2019 high mountain classification and false color vegetation index.*

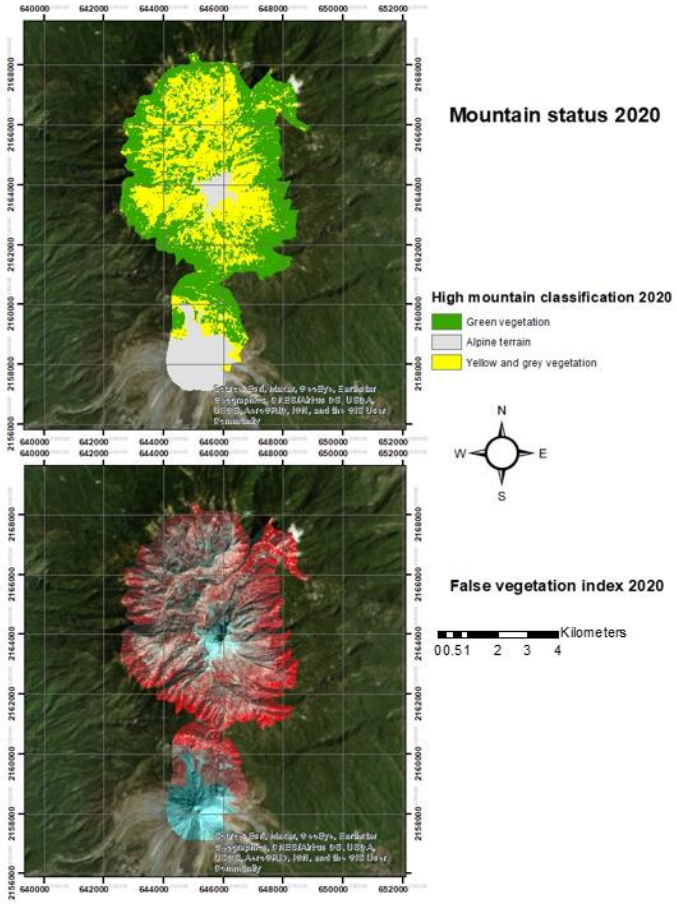


*Figure 34. 2020 high mountain classification and false color vegetation index.*

## Weather data:

## 2013:

| **2013** | | | | | |
|---|---|---|---|---|---|
| Month | Fortnight | Air temperature (degrees Celsius) | Relative Humidity (%) | Precipitation (mm) | Radiation (w/m2) |
| Jan | 1 | 7.0 | 57.7 | 28 | 230.1 |
| | 2 | 5.4 | 69.2 | 5.2 | 150.0 |
| Feb | 3 | 8.7 | 41.4 | 0 | 110.9 |
| | 4 | 9.1 | 35.3 | 0 | 276.7 |
| Mar | 5 | 6.9 | 43.4 | 7.8 | 225.3 |
| | 6 | 8.7 | 47.5 | 3.8 | 283.9 |
| Apr | 7 | 10.8 | 21.9 | 0 | 316.4 |
| | 8 | 12.2 | 30.0 | 0 | 330.0 |
| May | 9 | 11.2 | 35.3 | 0.6 | 290.6 |
| | 10 | 11.3 | 65.8 | 67.2 | 229.5 |
| Jun | 11 | 11.3 | 76.2 | 55.4 | 221.1 |
| | 12 | 8.9 | 90.7 | 97.8 | 154.3 |
| Jul | 13 | 8.1 | 88.9 | 207.8 | 162.3 |

| | | | | | |
|---|---|---|---|---|---|
| | 14 | 8.8 | 88.2 | 62.8 | 157.5 |
| Aug | 15 | 8.7 | 86.6 | 42 | 203.5 |
| | 16 | 8.4 | 90.6 | 143.4 | 179.1 |
| Sep | 17 | 8.6 | 95.5 | 536.2 | 142.2 |
| | 18 | 9.2 | 91.8 | 196.2 | 154.5 |
| Oct | 19 | 8.7 | 88.6 | 30.2 | 153.2 |
| | 20 | 8.4 | 84.9 | 18 | 156.6 |
| Nov | 21 | 7.2 | 89.6 | 49 | 141.6 |
| | 22 | 7.5 | 64.3 | 54 | 186.7 |
| Dec | 23 | 8.4 | 52.9 | 0 | 201.2 |
| | 24 | 5.4 | 76.8 | 121.6 | 132.9 |
| Annual precipitation (mm) | | | | 1727 | |

*Table 29. 2013 weather averages.*

## 2014:

| **2014** | | | | | |
|---|---|---|---|---|---|
| Month | Fortnight | Air temperature (degrees Celsius) | Relative Humidity (%) | Precipitation (mm) | Radiation (w/m2) |
| Jan | 1 | 4.4 | 68.2 | 3.4 | 146.6 |
| | 2 | 5.8 | 58.4 | 6.8 | 188.5 |
| Feb | 3 | 8.1 | 44.5 | 0 | 230.5 |
| | 4 | 8.4 | 48.0 | 0 | 233.7 |
| Mar | 5 | 8.3 | 37.3 | 0 | 279.5 |
| | 6 | 9.8 | 40.8 | 0 | 273.9 |
| Apr | 7 | 10.8 | 37.2 | 13.4 | 264.0 |
| | 8 | 9.9 | 55.1 | 10.6 | 220.0 |
| May | 9 | 9.8 | 65.8 | 61.4 | 231.1 |
| | 10 | 9.1 | 79.1 | 98.6 | 111.7 |
| Jun | 11 | 10.3 | 84.6 | 68.4 | 99.2 |
| | 12 | 9.2 | 92.4 | 116 | 41.5 |
| Jul | 13 | 8.6 | 92.0 | 96.4 | 118.7 |
| | 14 | 9.4 | 85.7 | 43.2 | 145.7 |
| Aug | 15 | 8.7 | 91.5 | 72.4 | 188.4 |
| | 16 | 8.9 | 90.7 | 49.8 | 180.1 |
| Sep | 17 | 8.2 | 97.3 | 274 | 132.6 |
| | 18 | 9.3 | 90.9 | 110.4 | 173.4 |
| Oct | 19 | 8.9 | 90.8 | 104.2 | 158.5 |
| | 20 | 8.6 | 77.1 | 10 | 207.9 |
| Nov | 21 | 7.0 | 85.0 | 158 | 144.1 |
| | 22 | 7.7 | 52.4 | 1.8 | 179.8 |
| Dec | 23 | 6.1 | 71.0 | 2.6 | 161.0 |
| | 24 | 6.7 | 54.7 | 0.8 | 190.1 |
| Annual precipitation (mm) | | | | 1302.2 | |

*Table 30. 2014 weather averages.*

## 2015:

| 2015 | | | | | |
|---|---|---|---|---|---|
| Month | Fortnight | Air temperature (degrees Celsius) | Relative Humidity (%) | Precipitation (mm) | Radiation (w/m2) |
| Jan | 1 | 5.4 | 64.0 | 0 | 158.1 |
| | 2 | 6.7 | 63.4 | 0.6 | 180.4 |
| Feb | 3 | 4.8 | 67.2 | 74.8 | 177.6 |
| | 4 | 8.6 | 48.4 | 18.8 | 263.5 |
| Mar | 5 | 5.7 | 65.9 | 177 | 201.1 |
| | 6 | 7.5 | 64.3 | 206.2 | 169.6 |
| Apr | 7 | 10.0 | 62.3 | 0 | 162.3 |
| | 8 | 10.1 | 54.2 | 0.2 | 174.0 |
| May | 9 | 10.7 | 62.0 | 4.8 | 193.6 |
| | 10 | 9.9 | 77.7 | 60.6 | 174.0 |
| Jun | 11 | 10.0 | 82.8 | 49 | 202.0 |
| | 12 | 9.0 | 87.6 | 82.8 | 141.6 |
| Jul | 13 | 7.9 | 90.3 | 106.6 | 143.3 |
| | 14 | 9.2 | 84.4 | 71.8 | 172.0 |
| Aug | 15 | 9.2 | 83.3 | 93.6 | 183.0 |
| | 16 | 9.1 | 84.4 | 76.8 | 185.4 |
| Sep | 17 | 9.0 | 89.2 | 45.8 | 161.6 |
| | 18 | 8.9 | 87.3 | 25.4 | 179.6 |
| Oct | 19 | 9.2 | 82.9 | 20.8 | 182.2 |
| | 20 | 9.1 | 83.0 | 544.6 | 166.0 |
| Nov | 21 | 9.5 | 75.2 | 6.4 | 214.6 |
| | 22 | 8.8 | 76.8 | 3.2 | 142.5 |
| Dec | 23 | 6.9 | 68.3 | 90.6 | 141.4 |
| | 24 | 8.7 | 46.4 | 0 | 194.8 |
| Annual precipitation (mm) | | | | 1760.4 | |

*Table 31. 2015 weather averages.*

## 2016:

| 2016 | | | | | |
|---|---|---|---|---|---|
| Month | Fortnight | Air temperature (degrees Celsius) | Relative Humidity (%) | Precipitation (mm) | Radiation (w/m2) |
| Jan | 1 | 6.1 | 39.9 | 30 | 209.1 |
| | 2 | 6.7 | 26.8 | 0 | 242.1 |
| Feb | 3 | 7.5 | 32.9 | 0 | 235.0 |
| | 4 | 9.1 | 42.7 | 0 | 244.2 |
| Mar | 5 | 5.9 | 46.3 | 15 | 249.4 |
| | 6 | 8.9 | 32.4 | 0 | 274.4 |
| Apr | 7 | 11.7 | 34.0 | 0 | 285.5 |
| | 8 | 9.9 | 33.5 | 0 | 225.6 |
| May | 9 | 12.2 | 55.6 | 19.8 | 207.8 |
| | 10 | 12.4 | 56.3 | 13.8 | 222.6 |
| Jun | 11 | 10.1 | 75.0 | 49 | 199.5 |

| | | | | | |
|---|---|---|---|---|---|
| | 12 | 8.8 | 89.2 | 112.2 | 171.5 |
| Jul | 13 | 8.6 | 87.1 | 117.8 | 170.9 |
| | 14 | 8.4 | 88.9 | 105.2 | 170.5 |
| Aug | 15 | 9.4 | 86.5 | 93.8 | 168.6 |
| | 16 | 8.5 | 91.0 | 108.2 | 22.9 |
| Sep | 17 | 9.3 | 88.4 | 341.6 | 0.2 |
| | 18 | 8.6 | 91.0 | 62.6 | 0.0 |
| Oct | 19 | 9.7 | 85.2 | 12.8 | 0.0 |
| | 20 | 8.0 | 79.1 | 18.6 | 0.0 |
| Nov | 21 | 7.0 | 87.7 | 204.6 | |
| | 22 | 6.9 | 74.1 | 0.4 | |
| Dec | 23 | 7.6 | 56.4 | 6 | 177.0 |
| | 24 | 6.9 | 74.0 | 12 | 156.1 |
| Annual precipitation (mm) | | | | 1323.4 | |

*Table 32. 2016 weather averages.*

## 2017:

| **2017** | | | | | |
|---|---|---|---|---|---|
| Month | Fortnight | Air temperature (degrees Celsius) | Relative Humidity (%) | Precipitation (mm) | Radiation (w/m2) |
| Jan | 1 | 7.4 | 44.2 | 0 | 184.5 |
| | 2 | 7.1 | 36.1 | 0 | 220.3 |
| Feb | 3 | 7.5 | 51.2 | 0.2 | 199.5 |
| | 4 | 6.2 | 44.8 | 12 | 275.4 |
| Mar | 5 | 6.6 | 70.7 | 32.6 | 167.1 |
| | 6 | 9.7 | 47.3 | 0 | 279.3 |
| Apr | 7 | 11.2 | 25.1 | 0 | 330.6 |
| | 8 | 10.4 | 32.2 | 0 | 268.4 |
| May | 9 | 11.5 | 43.1 | 1 | 220.8 |
| | 10 | 13.3 | 51.9 | 15 | 287.9 |
| Jun | 11 | 12.0 | 67.2 | 33.8 | 255.7 |
| | 12 | 10.2 | 83.4 | 117.6 | 191.1 |
| Jul | 13 | 8.4 | 91.7 | 119.4 | 146.1 |
| | 14 | 8.6 | 89.4 | 110.4 | 160.3 |
| Aug | 15 | 9.3 | 87.7 | 142.2 | 191.4 |
| | 16 | 9.1 | 91.3 | 271.8 | 175.1 |
| Sep | 17 | 8.9 | 90.9 | 93.8 | 189.8 |
| | 18 | 9.3 | 91.3 | 174 | 160.3 |
| Oct | 19 | 8.6 | 95.3 | 59.2 | 152.3 |
| | 20 | 8.4 | 74.6 | 2.6 | 207.4 |
| Nov | 21 | 9.8 | 61.4 | 0.4 | 248.1 |
| | 22 | 7.5 | 47.0 | 0 | 241.2 |
| Dec | 23 | 7.4 | 51.1 | 0 | 210.5 |
| | 24 | 5.7 | 71.9 | 36.2 | 165.8 |
| Annual precipitation (mm) | | | | 1222.2 | |

*Table 33. 2017 weather averages.*

## 2018:

| 2018 | | | | | |
|---|---|---|---|---|---|
| Month | Fortnight | Air temperature (degrees Celsius) | Relative Humidity (%) | Precipitation (mm) | Radiation (w/m2) |
| Jan | 1 | 6.2 | 56.0 | 0.6 | 207.8 |
| | 2 | 4.9 | 63.1 | 35.2 | 153.4 |
| Feb | 3 | 5.8 | 77.5 | 25 | 172.7 |
| | 4 | 7.2 | 72.7 | 0.2 | 152.5 |
| Mar | 5 | 9.9 | 46.4 | 0 | 278.8 |
| | 6 | 9.8 | 40.7 | 0 | 297.7 |
| Apr | 7 | 9.2 | 43.5 | 0 | 280.9 |
| | 8 | 11.0 | 54.4 | 0.2 | 261.9 |
| May | 9 | 9.3 | 82.4 | 80.2 | 187.1 |
| | 10 | 13.4 | 54.8 | 5.8 | 288.4 |
| Jun | 11 | 10.3 | 81.6 | 47.6 | 217.4 |
| | 12 | 8.5 | 92.8 | 94.6 | 157.7 |
| Jul | 13 | 8.3 | 91.5 | 106.4 | 157.6 |
| | 14 | 9.5 | 84.9 | 50.2 | 183.4 |
| Aug | 15 | 8.1 | 94.6 | 47.2 | 158.7 |
| | 16 | 8.4 | 91.6 | 81.8 | 199.8 |
| Sep | 17 | 8.5 | 94.9 | 102 | 176.5 |
| | 18 | 8.5 | 95.3 | 84.2 | 157.0 |
| Oct | 19 | 8.5 | 94.4 | 92.6 | 159.3 |
| | 20 | 8.0 | 93.0 | 176.4 | 122.7 |
| Nov | 21 | 6.7 | 83.1 | 80.8 | 136.8 |
| | 22 | 7.5 | 53.4 | 128.8 | 202.2 |
| Dec | 23 | 7.4 | 59.5 | 0 | 175.9 |
| | 24 | 6.6 | 34.6 | 1.6 | 204.0 |
| Annual precipitation (mm) | | | | 1241.4 | |

*Table 34. 2018 weather averages.*

## 2019:

| 2019 | | | | | |
|---|---|---|---|---|---|
| Month | Fortnight | Air temperature (degrees Celsius) | Relative Humidity (%) | Precipitation (mm) | Radiation (w/m2) |
| Jan | 1 | 6.9 | 62.3 | 4.6 | 170.0 |
| | 2 | 6.7 | 46.2 | 8.2 | 218.9 |
| Feb | 3 | 8.9 | 45.3 | 0 | 244.3 |
| | 4 | 9.0 | 45.1 | 2.2 | 248.5 |
| Mar | 5 | 11.0 | 43.0 | 0 | 272.9 |
| | 6 | 9.2 | 41.8 | 0 | 301.2 |
| Apr | 7 | 9.5 | 29.0 | 0 | 326.3 |
| | 8 | 11.7 | 36.1 | 0 | 312.4 |
| May | 9 | 12.4 | 27.6 | 0 | 325.0 |
| | 10 | 12.2 | 54.6 | 11.4 | 262.7 |
| Jun | 11 | 10.9 | 83.3 | 53.6 | 186.8 |
| | 12 | 10.2 | 83.7 | 26 | 177.5 |
| Jul | 13 | 8.9 | 89.7 | 0.4 | 180.9 |

| | | | | | |
|---|---|---|---|---|---|
| | 14 | 8.1 | 93.5 | 100.4 | 150.3 |
| Aug | 15 | 9.2 | 89.2 | 76.2 | 195.1 |
| | 16 | 9.4 | 90.7 | 74 | 196.6 |
| Sep | 17 | 8.5 | 92.5 | 141.6 | 151.5 |
| | 18 | 9.1 | 94.0 | 246.8 | 177.4 |
| Oct | 19 | 8.9 | 92.3 | 44 | 202.4 |
| | 20 | 8.4 | 85.9 | 130 | 151.0 |
| Nov | 21 | 7.2 | 95.3 | 64.4 | 133.1 |
| | 22 | 8.2 | 77.5 | 2.2 | 151.2 |
| Dec | 23 | 8.0 | 58.0 | 0 | 218.2 |
| | 24 | 5.9 | 68.6 | 12 | 178.0 |
| Annual precipitation (mm) | | | | 998 | |

*Table 35. 2019 weather averages.*

## 2020:

| **2020** | | | | | |
|---|---|---|---|---|---|
| Month | Fortnight | Air temperature (degrees Celsius) | Relative Humidity (%) | Precipitation (mm) | Radiation (w/m2) |
| Jan | 1 | 7.0 | 43.6 | 97 | 204.7 |
| | 2 | 5.9 | 65.7 | 5.2 | 165.0 |
| Feb | 3 | 6.7 | 58.6 | 135.4 | 171.0 |
| | 4 | 9.1 | 61.4 | 0 | 250.7 |
| Mar | 5 | 9.6 | 60.7 | 0.8 | 216.4 |
| | 6 | 10.6 | 57.8 | 0.2 | 264.4 |
| Apr | 7 | 11.0 | 37.1 | 0 | 324.1 |
| | 8 | 12.1 | 50.6 | 0.2 | 300.8 |
| May | 9 | 10.5 | 59.2 | 12.4 | 248.2 |
| | 10 | 11.9 | 37.8 | 58.6 | 303.2 |
| Jun | 11 | 11.5 | 78.0 | 35.2 | 239.4 |
| | 12 | 9.4 | 93.4 | 119.2 | 170.2 |
| Jul | 13 | 9.3 | 91.2 | 96.6 | 203.0 |
| | 14 | 9.1 | 92.3 | 130 | 172.9 |
| Aug | 15 | 9.0 | 95.5 | 140.4 | 178.8 |
| | 16 | 8.8 | 96.5 | 150.6 | 167.1 |
| Sep | 17 | 8.9 | 94.6 | 99.8 | 175.6 |
| | 18 | 9.0 | 90.7 | 84 | 194.9 |
| Oct | 19 | 8.7 | 68.1 | 17.6 | 244.3 |
| | 20 | 9.2 | 78.4 | 1.6 | 209.6 |
| Nov | 21 | 9.3 | 57.8 | 0 | 254.2 |
| | 22 | 8.7 | 71.8 | 1.6 | 192.7 |
| Dec | 23 | 6.9 | 69.6 | 8.6 | 190.1 |
| | 24 | 6.9 | 37.7 | 0 | 221.5 |
| Annual precipitation (mm) | | | | 1195 | |

*Table 36. 2020 weather averages.*

## Lab work:

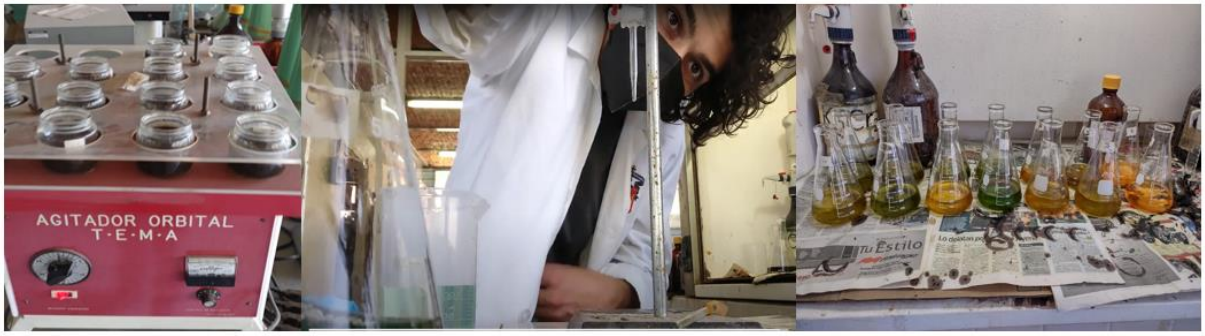


*Figure 35. Organic matter work.*

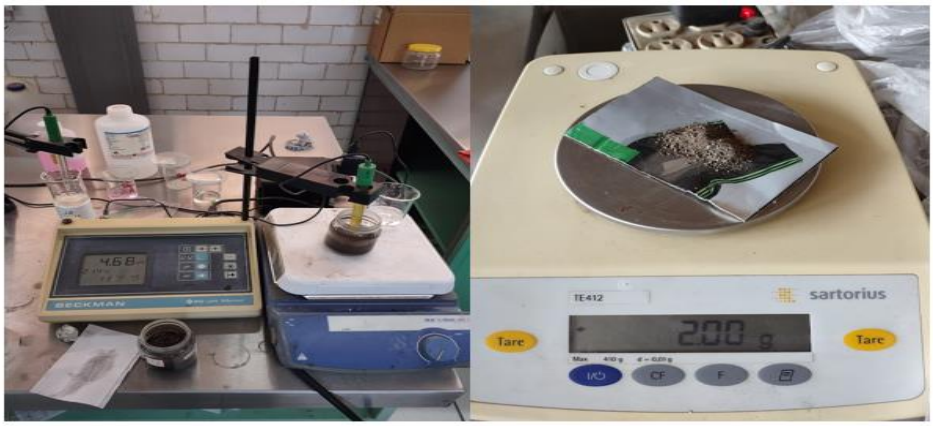


*Figure 36. pH and EC work.*

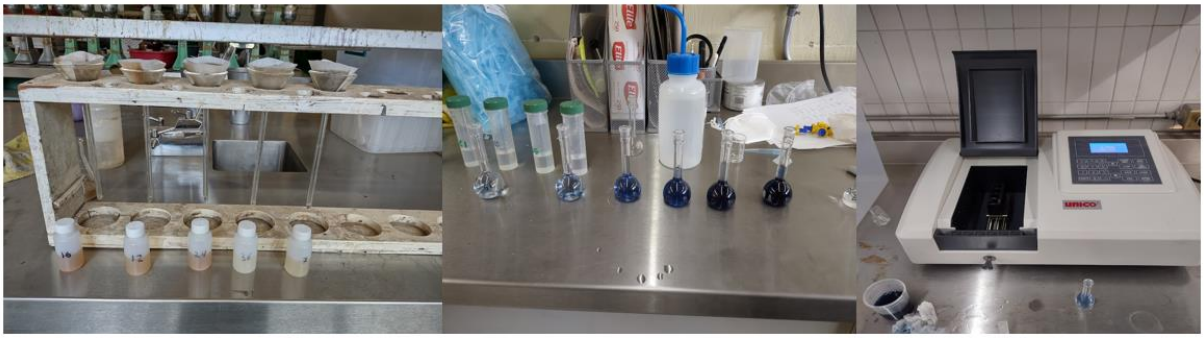

*Figure 37. Phosphorus work.*

*Figure 38. Nitrogen work.*

*Figure 39. Soil cations work.*

*Figure 40. Fun at Nevado de Colima peak.*